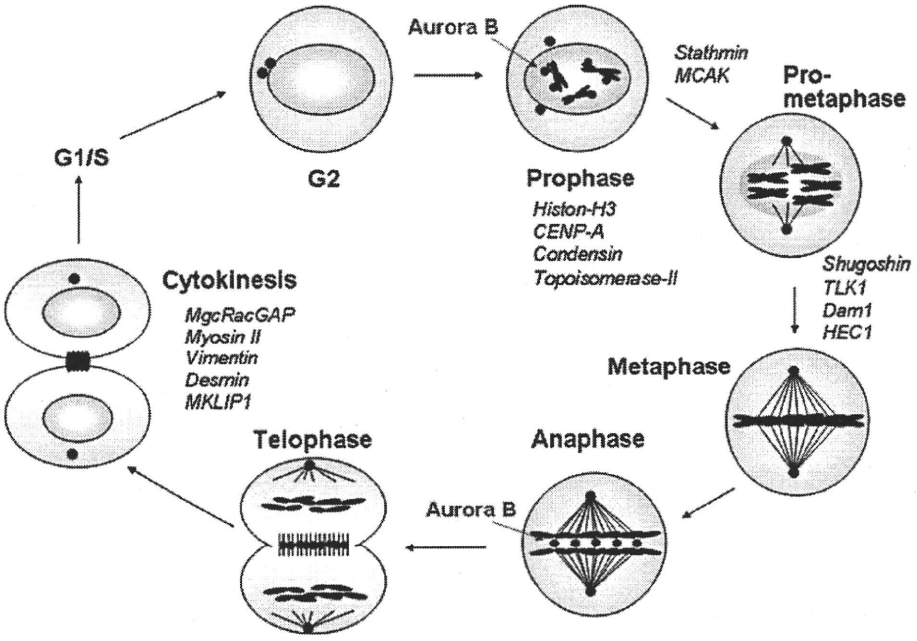

Fig. 4 Mitosis phase of the cell cycle. Localization of Aurora kinase B indicated by *arrows*. Main substrates of Aurora kinase B shown in *italics*

recurrence of HCC even after curative hepatectomy [37]. Array-CGH revealed the CIN phenotype of HCC was closely related to Aurora kinase B expression. Aurora kinase B is a chromosomal passenger protein that regulates accurate chromosomal segregation, cytokinesis, protein localization to the centromere and kinetochore, correct microtubule-kinetochore attachments, and regulation of the mitotic checkpoint (Fig. 4) [38]. Recent studies revealed that deregulation of Aurora kinase B directly caused CIN and aneuploidy, transforming epithelial cells [39].

More important, several small-molecule inhibitors of Aurora kinase have been developed as anti-cancer agents including ZM447439, VX-680, PHA-680632, AZD1152 and MLN 8054 [40]. In particular, Aurora kinase B may be a suitable anticancer target, because inhibition of Aurora kinase B rapidly results in catastrophic mitosis with senescence. In our studies to evaluate the effects of Aurora B inhibitor on human HCC, accumulation of polyploidy and apoptosis was observed in all of the cell lines after administration of the inhibitor [41]. We utilized a novel orthotopic xenograft model of liver tumors to explore tumor growth inhibition in situ. Aurora B inhibitor was administered to mice bearing human HCC orthotopic xenografts. Growth of liver tumors was found to be suppressed in all of the mice that had been treated with the Aurora B inhibitor. After drug administration, the mean liver tumor weight in those animals that had received Aurora B inhibitor was 10% of that in the control mice. Similar growth inhibition was observed in orthotopic xenografts using other HCC cell lines after administration of Aurora B inhibitor. In the orthotopic model, mice survival was significantly enhanced by Aurora B inhibitor treatment in comparison with the control. All of the host tissues examined, including liver, bone marrow, kidney, intestine, and lung, were histologically normal in all experiments. Specific inhibition of Aurora kinases is a promising novel therapeutic approach for treatment of aggressive HCC [42].

"Synthetic lethality", a novel strategy for molecularly targeted therapy

These mitotic kinases have been recognized as promising molecular targets—"Achilles' heels" of various malignancies [3]. More recently, another mitotic kinase, PLK1, was identified as a specific molecule with synthetic lethal interactions with mutant Ras oncogenes in cancer cells [43] (Fig. 5a). "Synthetic lethality" is a concept from traditional genetic science on drosophila, first described by Dobzhansky in 1946 [44]. As shown in Fig. 5b, two genes ("A" and "B") are said to be in a "synthetic lethal" relationship if a mutation in either gene alone is not lethal but mutations in both cause the death of the cell. This concept can be extended to situations in discovery of molecular targets [45]. In applying synthetic lethality to the discovery of agents targeting cancer cells, a screening program is designed to find a target gene that kills cells bearing a cancer-specific alteration, such as a mutated tumor-suppressor gene or an activated oncogene, but spares otherwise identical cells lacking the cancer-specific alteration. Such a gene can then be the target for developing an anticancer drug.

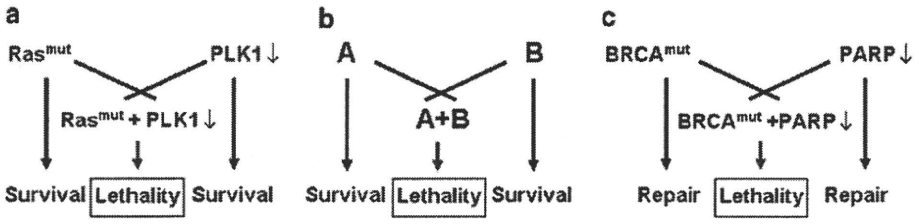

Fig. 5 The concept of synthetic lethality. Synthetic lethal interactions were demonstrated with mutant Ras and PLK1 inhibition (**a**), the fundamental pattern of mutations *A* and *B* (**b**), and mutant BRCA and PARP inhibitor applied clinically (**c**)

In such screening programs for synthetic lethality to identify druggable targets that are unique to tumor cells but not normal cells [45], one successful and hopeful example has already been published as a phase I clinical trial of poly(ADP-ribose) polymerase 1 (PARP1) inhibitors in patients with hereditary breast and ovarian carcinomas with mutated BRCAs [46] (Fig. 5c). BRCA1 and BRCA2 are tumor-suppressor genes that are key participants in homologous recombination to repair DNA damage [47]. The enzyme activity of poly(ADP-ribose) polymerase 1 (PARP1) is required for base-excision repair, a DNA-damage repair pathway that recognizes and eliminates DNA bases damaged by oxidation in a process during each normal cell cycle. Normally, homologous recombination repairs these breaks, whereas in the case of absent BRCA1 or BRCA2, the cell dies without repair of the breaks. As predicted by the concept of synthetic lethality, small molecule inhibitors of PARP1 are toxic to cells deficient in BRCA1 or BRCA2, whereas cells in which BRCA1 or BRCA2 is restored are less sensitive to the inhibitors [48, 49]. According to these actual proofs with clinical benefits, the concept of synthetic lethality should be expanded not only to identification of novel druggable molecules but also to the rationale of addictions to oncogene and non-oncogene as the therapeutic targets. Further application of this synthetic lethal strategy must be actively engaged in developing a novel targeted therapy of HCC.

Conclusion

HCC is one of the most common malignancies worldwide, and the incidence is still increasing [50]. The primary curative treatment for HCC is surgical resection, and there has been limited improvement in the availability of alternative treatments in the last decade [51]. Because there is an urgent need to develop novel treatments for HCC, the bench-to-bedside translational approach should be implemented more intensely to elucidate the molecular mechanisms and therapeutic targets of advanced and/or recurrent HCC [52].

Conflict of interest statement No author has any conflict of interest.

References

1. Hanahan D, Weinberg RA (2000) The hallmarks of cancer. Cell 100(1):57–70
2. Kroemer G, Pouyssegur J (2008) Tumor cell metabolism: cancer's Achilles' heel. Cancer Cell 13(6):472–482
3. Luo J, Solimini NL, Elledge SJ (2009) Principles of cancer therapy: oncogene and non-oncogene addiction. Cell 136(5):823–837
4. Weinstein IB (2002) Cancer. addiction to oncogenes-the Achilles heal of cancer. Science 297(5578):63–64
5. Weinstein IB, Joe AK (2006) Mechanisms of disease: oncogene addiction—a rationale for molecular targeting in cancer therapy. Nat Clin Pract Oncol 3(8):448–457
6. Tanaka S, Arii S (2009) Molecularly targeted therapy for hepatocellular carcinoma. Cancer Sci 100(1):1–8
7. Llovet JM, Bruix J (2008) Molecular targeted therapies in hepatocellular carcinoma. Hepatology 48:1312–1327
8. Yau T, Chan P, Epstein R et al (2009) Management of advanced hepatocellular carcinoma in the era of targeted therapy. Liver Int 29(1):10–17 Review
9. Hanahan D, Folkman J (1996) Patterns and emerging mechanisms of the angiogenic switch during tumorigenesis. Cell 86:353–364
10. Tanaka S, Arii S (2006) Current status of perspective of antiangiogenic therapy for cancer; hepatocellular carcinoma. Int J Clin Oncol 11:82–89
11. Ferrara N (2002) VEGF and the quest for tumour angiogenesis factors. Nat Rev Cancer 2(10):795–803
12. Mise M, Arii S, Higashituji H et al (1996) Clinical significance of vascular endothelial growth factor and basic fibroblast growth factor gene expression in liver tumor. Hepatology 23(3):455–464
13. Schmitt M, Horbach A, Kubitz R et al (2004) Disruption of hepatocellular tight junctions by vascular endothelial growth factor (VEGF): a novel mechanism for tumor invasion. J Hepatol 41(2):274–283
14. Kaplan RN, Riba RD, Zacharoulis S et al (2005) VEGFR1-positive haematopoietic bone marrow progenitors initiate the premetastatic niche. Nature 438(7069):820–827
15. Hiratsuka S, Watanabe A, Aburatani H et al (2006) Tumour-mediated upregulation of chemoattractants and recruitment of myeloid cells predetermines lung metastasis. Nat Cell Biol 8(12):1369–1375
16. Arii S (2004) Role of vascular endothelial growth factor on the invasive potential of hepatocellular carcinoma. J Hepatol 41(2):333–335

17. Andrae J, Gallini R, Betsholtz C (2008) Role of platelet-derived growth factors in physiology and medicine. Genes Dev 22(10):1276–1312
18. Kuhnert F, Tam BY, Sennino B et al (2008) Soluble receptor-mediated selective inhibition of VEGFR and PDGFRbeta signaling during physiologic and tumor angiogenesis. Proc Natl Acad Sci USA 105(29):10185–10190
19. Uematsu S, Higashi T, Nouso K et al (2005) Altered expression of vascular endothelial growth factor, fibroblast growth factor-2 and endostatin in patients with hepatocellular carcinoma. J Gastroenterol Hepatol 20(4):583–588
20. Poon RT, Ng IO, Lau C et al (2001) Correlation of serum basic fibroblast growth factor levels with clinicopathologic features and postoperative recurrence in hepatocellular carcinoma. Am J Surg 182:298–304
21. Llovet JM, Ricci S, Mazzaferro V et al (2008) Sorafenib in advanced hepatocellular carcinoma. N Engl J Med 359:378–390
22. Tanaka S, Mori M, Sakamoto Y et al (1999) Biologic significance of angiopoietin-2 expression in human hepatocellular carcinoma. J Clin Investig 103(3):341–345
23. Tanaka S, Wands JR, Arii S (2006) Induction of angiopoietin-2 gene expression by COX-2: A novel role for COX-2 inhibitors during hepatocarcinogenesis. J Hepatol 44(1):233–235
24. Tanaka S, Sugimachi K, Yamashita Yi et al (2002) Tie2 vascular endothelial receptor expression and function in hepatocellular carcinoma. Hepatology 35(4):861–867
25. Seegar TC, Eller B, Tzvetkova-Robev D et al (2010) Tie1–Tie2 interactions mediate functional differences between angiopoietin ligands. Mol Cell 37(5):643–655
26. Holash J, Maisonpierre PC, Compton D et al (1999) Vessel cooption, regression, and growth in tumors mediated by angiopoietins and VEGF. Science 284(5422):1994–1998
27. Oliner J, Min H, Leal J et al (2004) Suppression of angiogenesis and tumor growth by selective inhibition of angiopoietin-2. Cancer Cell 6(5):507–516
28. Herbst RS, Hong D, Chap L et al (2009) Safety, pharmacokinetics, and antitumor activity of AMG 386, a selective angiopoietin inhibitor, in adult patients with advanced solid tumors. J Clin Oncol 27(21):3557–3565
29. Pawson T (2004) Specificity in signal transduction: from phosphotyrosine–SH2 domain interactions to complex cellular systems. Cell 116:191–203
30. Tanaka S, Sugimachi K, Maehara S et al (2002) Oncogenic signal transduction and therapeutic strategy for hepatocellular carcinoma. Surgery 131:S142–S147
31. Schagdarsurengin U, Wilkens L, Steinemann D et al (2003) Frequent epigenetic inactivation of the RASSF1A gene in hepatocellular carcinoma. Oncogene 22:1866–1871
32. Farazi PA, DePinho RA (2006) Hepatocellular carcinoma pathogenesis: from genes to environment. Nat Rev Cancer 6:674–687
33. Luo J, Manning BD, Cantley LC (2003) Targeting the PI3K-Akt pathway in human cancer: rationale and promise. Cancer Cell 4:257–262
34. Chiang GG, Abraham RT (2007) Targeting the mTOR signaling network in cancer. Trends Mol Med 13:433–442
35. Foster KG, Fingar DC (2010) mTOR: conducting the cellular signaling symphony. J Biol Chem
36. Schvartzman JM, Sotillo R, Benezra R (2010) Mitotic chromosomal instability and cancer: mouse modelling of the human disease. Nat Rev Cancer 10(2):102–115
37. Tanaka S, Arii S, Yasen M et al (2008) Aurora kinase B is a predictive factor for the aggressive recurrence of hepatocellular carcinoma after curative hepatectomy. Br J Surg 95:611–619
38. Keen N, Taylor S (2004) Aurora-kinase inhibitors as anticancer agents. Nat Rev Cancer 4:927–936
39. Nguyen HG, Makitalo M, Yang D et al (2009) Deregulated Aurora-B induced tetraploidy promotes tumorigenesis. FASEB J 23(8):2741–2748
40. Harrington EA, Bebbington D, Moore J et al (2004) VX-680, a potent and selective small-molecule inhibitor of the Aurora kinases, suppresses tumor growth in vivo. Nat Med 10(3):262–267
41. Aihara A, Tanaka S, Yasen M et al (2010) The selective Aurora B kinase inhibitor AZD1152 as a novel treatment for hepatocellular carcinoma. J Hepatol 52(1):63–71
42. Tanaka S, Mogushi K, Yasen M et al (2010) Gene-expression phenotypes for vascular invasiveness of hepatocellular carcinomas. Surgery 147(3):405–414
43. Luo J, Emanuele MJ, Li D et al (2009) A genome-wide RNAi screen identifies multiple synthetic lethal interactions with the Ras oncogene. Cell 137(5):835–848
44. Dobzhansky T (1946) Genetics of natural populations. XIII. Recombination and variability in populations of *Drosophila pseudoobscura*. Genetics 31:269–290
45. Kaelin WG Jr (2005) The concept of synthetic lethality in the context of anticancer therapy. Nat Rev Cancer 5(9):689–698
46. Fong PC, Boss DS, Yap TA et al (2009) Inhibition of poly(ADP-ribose) polymerase in tumors from BRCA mutation carriers. N Engl J Med 361(2):123–134
47. Iglehart JD, Silver DP (2009) Synthetic lethality—a new direction in cancer-drug development. N Engl J Med 361(2):189–191
48. Bryant HE, Schultz N, Thomas HD et al (2005) Specific killing of BRCA2-deficient tumours with inhibitors of poly(ADP-ribose) polymerase. Nature 434(7035):913–917
49. Farmer H, McCabe N, Lord CJ et al (2005) Targeting the DNA repair defect in BRCA mutant cells as a therapeutic strategy. Nature 434(7035):917–921
50. Ince N, Wands JR (1999) The increasing incidence of hepatocellular carcinoma. N Engl J Med 340:798–799
51. Arii S, Yamaoka Y, Futagawa S et al (2000) Results of surgical and nonsurgical treatment for small-sized hepatocellular carcinomas: a retrospective and nationwide survey in Japan. The Liver Cancer Study Group of Japan. Hepatology 32:1224–1229
52. Tanaka S, Arii S (2010) Medical treatments: in association or alone, their role and their future perspectives: novel molecular-targeted therapy for hepatocellular carcinoma. J Hepatobiliary Pancreat Surg

Research Article

EASL EUROPEAN ASSOCIATION FOR THE STUDY OF THE LIVER | JOURNAL OF HEPATOLOGY

The selective Aurora B kinase inhibitor AZD1152 as a novel treatment for hepatocellular carcinoma

Arihiro Aihara, Shinji Tanaka*, Mahmut Yasen, Satoshi Matsumura, Yusuke Mitsunori, Ayano Murakata, Norio Noguchi, Atsushi Kudo, Noriaki Nakamura, Koji Ito, Shigeki Arii

Department of Hepato-Biliary-Pancreatic Surgery, Graduate School of Medicine, Tokyo Medical and Dental University, 1-5-45 Yushima, Bunkyo-ku, Tokyo 113-8519, Japan

Background & Aims: We previously identified that high Aurora B expression was associated with hepatocellular carcinoma (HCC) recurrence due to tumor dissemination. In this preclinical study, a novel inhibitor of Aurora B kinase was evaluated as a treatment for human HCC.

Methods: AZD1152 is a selective inhibitor of Aurora B kinase. Twelve human HCC cell lines were analyzed for Aurora B kinase expression and the *in vitro* effects of AZD1152. The *in vivo* effects of AZD1152 were analyzed in a subcutaneous xenograft model and a novel orthotopic liver xenograft model.

Results: Aurora B kinase expression varied among the human HCC cell lines and was found to correlate with inhibition of cell proliferation, accumulation of 4N DNA, and the proportion of polyploid cells following administration of AZD1152-hydroxyquinazoline-pyrazol-anilide (AZD1152-HQPA). AZD1152-HQPA suppressed histone H3 phosphorylation and induced cell death in a dose-dependent manner. Growth of subcutaneous human HCC xenografts was inhibited by AZD1152 administration. In an orthotopic hepatoma model, treatment with AZD1152 significantly decelerated tumor growth and increased survival. Pharmacobiological analysis revealed that AZD1152 induced the rapid suppression of phosphohistone H3, followed by cellular apoptosis in the liver tumors but not in the normal tissues of the orthotopic models.

Conclusions: Our preclinical studies indicate that AZD1152 is a promising novel therapeutic approach for the treatment of HCC.

Introduction

Hepatocellular carcinoma (HCC) is one of the most common malignancies worldwide, accounting nearly for 1 million deaths per year [1], and the incidence is still increasing [2]. The primary curative treatment for HCC is surgical resection, and there has been limited improvement in the availability of alternative treatments in the last decade [3]. A major obstacle for the treatment of HCC is the high frequency of tumor recurrence after curative resection. In fact, it is the recurrence pattern, rather than the recurrence itself, that critically affects patient prognosis [4]. The systemic treatment of HCC using conventional anticancer agents has provided little clinical benefit or prolonged survival for patients with advanced HCC [5]. A recent clinical trial by Llovet et al. [6] revealed a molecular-targeted inhibitor, sorafenib, as the first agent that demonstrated an improved overall survival in patients with advanced HCC. The increased understanding of the molecular mechanisms regulating cancer progression has led to the development of novel targeted therapies [7,8]. In order to fulfill this promise, there is an urgent need to identify the optimal targets for treatment.

In our previous studies in HCC patients after curative resection, the aggressive recurrence exceeding Milan criteria showed extremely poor prognosis [9]; moreover, a genome wide microarray profiling analysis identified the over-expression of Aurora B kinase as the only independent factor predictive of the aggressive recurrence [10]. The Aurora kinase family of serine–threonine kinases control chromosome assembly and segregation during mitosis. Aberrant expression of the Aurora kinases has been reported in a variety of solid tumors including prostate [11], colon [12], pancreas [13], lung [14], breast [15], and thyroid [16]. These findings have led to an interest in these kinases as molecular targets for cancer treatment [17,18]. Several small-molecule inhibitors of Aurora kinases have been developed as potential anticancer treatments. According to the recent review on Aurora inhibitors [19], ZM447439, Hesperadin, and MK0457/VX680 were the first to be described and to have similar potency versus Aurora A, Aurora B, and Aurora C. Currently, MLN8054 and MLN8237 are being developed as selective Aurora A kinase inhibitors. AZD1152 is a selective inhibitor of Aurora kinase activity with specificity for Aurora B kinase [20,21]. AZD1152 is a prodrug that is rapidly converted to the active moiety AZD1152-hydroxyquinazoline-pyrazol-anilide (AZD1152-HQPA) in plasma. Thus, AZD1152 is used for *in vivo* studies, while AZD1152-HQPA is used for *in vitro* work.

The importance of the role of the organ microenvironment in cancer is being increasingly understood [22]. This is particularly true for HCC, an organotropic cancer in which the liver-specific

Keywords: Hepatocellular carcinoma; Aurora B kinase; AZD1152; Orthotopic model; Molecular-targeted agent.
Received 9 April 2009; received in revised form 2 July 2009; accepted 13 July 2009; available online 29 October 2009
*Corresponding author. Tel.: +81 3 58035928; fax: +81 3 58035264.
E-mail address: shinji.msrg@tmd.ac.jp (S. Tanaka).
Abbreviations: cCasp-3, cleaved caspase-3; HE, hematoxylin and eosin; HCC, hepatocellular carcinoma; HQPA, hydroxyquinazoline-pyrazol-anilide; IC_{50}, half-maximal inhibitory concentration; PBS, phosphate-buffered saline; PhH3, phosphohistone H3.

microenvironment may play a critical role in HCC tumor development, cellular apoptosis, and drug sensitivity [23]. Additionally, hepatic tumors reside within the liver parenchyma, where drug metabolism and transformation occur. Thus, the pharmacodynamics of drug therapy for intrahepatic tumors may vary significantly from those drugs targeted at tumors in peripheral tissues. Several attempts have been made to generate a model of intrahepatic HCC via intraportal or intrahepatic injection of tumor cells in mice; however, frequent cancer dissemination makes it particularly difficult to generate a single quantitative tumor. A recent report describes development of a novel orthotopic liver tumor xenograft model that could be used in quantitative investigations of a single tumor within its native microenvironment [24]. This might provide a system in which the tumor's biological response to therapeutic agents more closely mimics that observed in liver tumors in patients [25]. The *in vivo* efficacy of Aurora kinase inhibitors in orthotopic xenograft models of solid cancers has not been reported to date [20,26,27].

Outcome of HCC patients is determined by combination of two distinct types of HCC recurrence, and the aggressive recurrence is driven by malignant characteristics of the tumor [4,9]. Because Aurora B kinase was found to be associated with the aggressive recurrence exceeding Milan criteria [10], it makes sense to target Aurora B kinase to treat the tumor. In this regard, the Aurora B kinase-specific inhibitor AZD1152 might be an attractive candidate for HCC therapy. This investigation evaluates the *in vitro* and *in vivo* effects and pharmacodynamics of AZD1152 in a number of preclinical liver tumor models, including an orthotopic model that more closely mimics the human disease.

Materials and methods

Reagents

AZD1152-HQPA and its prodrug AZD1152 were provided by AstraZeneca Pharmaceuticals (Macclesfield, UK).

Cell culture

The human HCC cell lines SK-Hep1, Hep3B, and PLC/PRF/5 were obtained from the American Type Culture Collection (Manassas, VA, USA). Other human HCC cell lines—JHH-1, JHH-2, JHH-4, HuH-1, HuH-6, HuH-7, HLE, HLF, and HepG2—were obtained from the Human Science Research Resources Bank (Osaka, Japan). Culture media were RPMI-1640 (SK-Hep1, Hep3B, HuH-7, and HepG2), Dulbecco's modified Eagle's medium (PLC/PRF/5, HuH-1, HuH-6, HLE, and HLF), and William's E medium (JHH-1, JHH-2, and JHH-4), supplemented with 5% fetal bovine serum (FBS) for HLF cells or 10% FBS for the remaining cell lines. All media supplemented 100 U/mL of penicillin and 100 μg/mL of streptomycin; all cell lines were cultivated in a humidified incubator at 37 °C in 5% carbon dioxide and harvested with 0.25% trypsin–0.03% EDTA.

Analysis of cell proliferation and cell viability

All cell lines were cultured in logarithmic growth phase in the presence of various concentrations of AZD1152-HQPA (0.3–1000 nM) for 72 h. Cells were seeded at 4×10^4 cells in six-well plates with the appropriate control medium. After 24 h, plates were treated with compound and incubated for 72 h at 37 °C. At the end of the incubation time, cells were detached from each plate, and viable cells were counted using a hemocytometer. Half-maximal inhibitory concentration (IC_{50}) values were calculated with BioDataFit v.1.02 software using the four-parameter logistic model. The mean values and standard deviations of IC_{50} were calculated in triplicate for each cell line. To investigate cell viability, triplicate samples of SK-Hep1, Hep3B, and HLF cells were cultured in the presence of various concentrations of AZD1152-HQPA (1–100 nM) for 72 h. The number of nonviable cells was assessed using a hemocytometer and trypan blue dye exclusion.

Western blotting

Total protein was extracted from each cell line, as described previously [28]. Protein levels of Aurora B kinase, phosphohistone H3 (PhH3), and alpha-tubulin (control) were detected using standard western blot analysis on 8–15% sodium dodecyl sulfate polyacrylamide gel electrophoresis (SDS–PAGE). Blots were incubated overnight at 4 °C with the primary antibody antihuman Aurora B (1:1000; Abcam, Cambridge, UK; Catalog No. ab2254) or antihuman PhH3 (1:200; Santa Cruz, CA, USA; Catalog No. sc-8656-R), then at room temperature for 1 h with anti-alpha-tubulin (1:5000; Sigma–Aldrich, St. Louis, MO, USA; Catalog No. T9026). Appropriate secondary antibodies were added for 2 h, and protein expression was visualized with enhanced chemiluminescence by the ECL western blotting detection system (GE Healthcare, Buckinghamshire, UK). The expression ratio of Aurora B kinase to the control was analyzed using Multi-Gage software (FUJIFILM, Tokyo, Japan).

Flow cytometry

Samples of all cell lines in logarithmic growth phase were exposed to AZD1152-HQPA 100 nM for 24 h, and then fixed in 70% ethanol at −20 °C overnight. Cells were rehydrated in phosphate-buffered saline (PBS), and then resuspended in PBS containing RNase 100 μg/mL (Sigma) and propidium iodide 10 μg/mL. Cellular DNA content was analyzed on a FACS Caliber flow cytometer (Becton & Dickinson Biosciences, San Jose, CA, USA). For detection of apoptosis, cells were labeled with the Annexin V-FITC Kit (Miltenyi Biotec, Bergisch Gladbach, Germany; Catalog No. 130-092-052) at room temperature for 15 min, followed by analysis on a FACS Caliber flow cytometer.

Immunocytochemistry and immunohistochemistry

SK-Hep1, Hep3B, and HLF cells were cultured on glass slides coated with silane in the presence of various concentrations of AZD1152-HQPA (1–100 nM) for 4 h. They were then fixed using 3.7% formalin for 10 min and permeabilized using 100% methanol for 20 min for immunocytochemical detection of PhH3.

Xenograft tumor tissue was harvested, formalin fixed, and paraffin embedded. The primary antibodies, PhH3 (Upstate Cell Signaling Solution, Danvers, MA, USA; Catalog No. 9701) and anti-cleaved caspase-3 (anti-cCasp-3; Upstate Cell Signaling Solution; Catalog No. 9661), were used at 1:100 and 1:400 dilution, respectively, in PBS containing 1% bovine serum albumin. The tissue sections and slides were stained with an automated immunostainer (BenchMark XT; Ventana Medical Systems, Tucson, AZ, USA) using heat-induced epitope retrieval and a standard diaminobenzidine detection kit (Ventana).

In vivo studies in a subcutaneous tumor xenograft model

A subcutaneous tumor model was used to analyze the *in vivo* activity of AZD1152, as described previously [29]. Five-week-old female nude mice (nu/nu) were purchased from Japan SLC (Shizuoka, Japan) and kept under pathogen-free conditions, fed standard food, and given free access to sterilized water. In all experiments, mice were anesthetized by 100 mg/kg Nembutal intraperitoneal injection. Subcutaneous xenografts were established by inoculating 1×10^7 SK-Hep1 cells into the right dorsal flank. Palpable tumors were confirmed on day 5 following inoculation, and mice were randomized into treatment groups to receive AZD1152 or the control Tris-buffered saline. AZD1152 was prepared in Tris-buffered saline (pH 9) and administered by intraperitoneal injection. Tumor size was measured using calipers as frequently as every other day for 2 weeks, and tumor volumes were calculated as $AB^2 \times 0.5$ (A, length; B, width). The Animal Care Committee of Tokyo Medical and Dental University School of Medicine approved the experimental protocols in accordance with its institutional guidelines.

In vivo studies in a novel orthotopic xenograft model

An orthotopic xenograft model was created by direct intrahepatic inoculation of SK-Hep1 and Hep3B cells, as described by Lu et al. [25]. With the mice fully anesthetized, a small transverse incision was made below the sternum to expose the liver. Then, 2.5×10^6 cells suspended in 25 μL of RPMI-1640 and 25 μL of Matrigel (Becton & Dickinson Biosciences) were slowly injected at a 30° angle into the upper left lobe of the liver using a 28-gauge needle. After injection, a small piece of sterile gauze was placed on the injection site, and light pressure was applied for 1 min to prevent bleeding. The abdomen was then closed with a 6–0 silk suture. Pilot studies confirmed development of liver tumors in 6 of 6 mice at

14 days after inoculation. AZD1152 (100 mg/kg) or the control Tris buffer was administered to mice by intraperitoneal injection on 2 consecutive days per week for 2 weeks starting on day 14 after inoculation. In both cell lines at 4 weeks after initiation of treatment, mice were sacrificed to assess the antitumor effects of AZD1152. The survival end points were defined as ascites formation in the hepatoma-bearing mice [30]. Animal survival data were entered in the Kaplan–Meier Life Table format and presented as the cumulative survival plot. Statistical differences were analyzed by Mantel–Cox log-rank test. All *in vivo* procedures were approved by the Animal Care Committee of Tokyo Medical and Dental University (Permission No. 090235).

The pharmacobiological effects of AZD1152 treatment in the orthotopic liver tumors were assessed by immunohistochemical analysis of PhH3 and cCasp-3 expression in control tumors and in those harvested 3 and 5 days after initiation of AZD1152 treatment.

Results

Aurora B kinase expression and in vitro effects of AZD1152-HQPA in human hepatocellular carcinoma cells

Evaluation of Aurora B kinase protein in 12 human HCC cell lines revealed a variety of expression levels, as shown in Fig. 1A (Aurora B/tubulin expression ratio: JHH-1, 0.120; JHH-2, 0.039; JHH-4, 0.059; HuH-1, 0.078; HuH-6, 0.220; HuH-7, 0.243; HLE, 0.040; HLF, 0.032; PLC/PRF/5, 0.083; SK-Hep1, 0.107; Hep3B, 0.079; HepG2, 0.044). Expression of Aurora B kinase was approximately 7-fold higher in HuH-7 and HuH-6 cells than in JHH-2 and HLF cells. To evaluate the growth inhibitory effects of AZD1152-HQPA, cell proliferation assays were conducted in these HCC cell lines. AZD1152-HQPA showed potent antiproliferative activity in all HCC cell types with IC_{50} values (JHH-1, 17.4 ± 1.0 nM; JHH-2, 218.0 ± 10.8 nM; JHH-4, 155.6 ± 16.8 nM; HuH-1, 27.3 ± 5.0 nM; HuH-6, 3.7 ± 0.6 nM; HuH-7, 6.8 ± 0.3 nM; HLE, 45.9 ± 6.4 nM; HLF, 126.1 ± 12.2 nM; PLC/PRF/5, 76.9 ± 9.9 nM; SK-Hep1, 21.9 ± 1.2 nM; Hep3B, 7.6 ± 1.2 nM; HepG2, 14.7 ± 1.7 nM) (Fig. 1A). Fig. 1B demonstrates the relationship between Aurora B kinase expression and indexes of AZD1152-HQPA IC_{50} in the panel of cell lines tested (correlation coefficient: −0.72738; $R^2 = 0.529$; $p = 0.0073$).

Alterations in DNA ploidy in the human HCC cell lines were analyzed by flow cytometry (Fig. 1C). Accumulation of cells with >4N DNA content was observed in all of the cell lines following

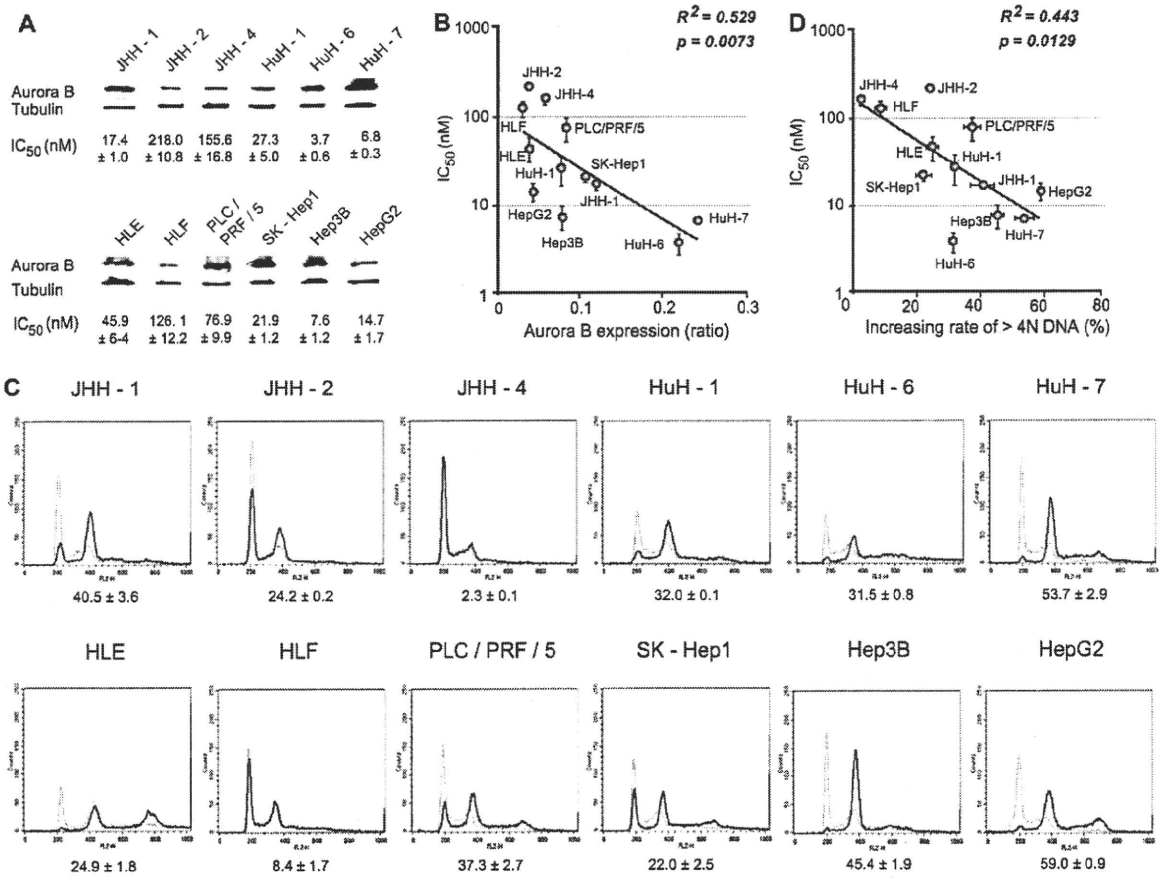

Fig. 1. Expression of Aurora B kinase and AZD1152-hydroxyquinazoline-pyrazol-anilide (AZD1152-HQPA) activity in human hepatocellular carcinoma (HCC) cell lines. (A) Western blot analysis of Aurora B kinase and the control alpha-tubulin. The concentration that induced half-maximal inhibitory concentration (IC_{50}) in 12 human HCC cell lines is indicated. (B) Relationship between the ratio of Aurora B kinase expression to control tubulin and the indexes of AZD1152 IC_{50} values in each human HCC cell line. Correlations were analyzed by Pearson two-tailed correlation. The level of statistical significance was $p < 0.05$. (C) Cellular DNA content was analyzed by flow cytometry in 12 human HCC cell lines after 24-h incubation with AZD1152-HQPA 100 nM (thick lines) or the control DMSO buffer (thin lines), and the increasing rate of >4N DNA (%) was indicated. (D) Relationship between the increasing rate of >4N cells and the indexes of AZD1152 IC_{50} values in each human HCC cell line. Correlations were analyzed by Pearson two-tailed correlation. The level of statistical significance was $p < 0.05$.

24-h incubation with AZD1152-HQPA 100 nM, with the exception of JHH-2 and HLF, which showed AZD1152 insensitivity with low expression levels of Aurora B kinase. As shown in Fig. 1D, the increasing rate of >4N DNA by AZD1152-HQPA (JHH-1, 40.5 ± 3.6%; JHH-2, 24.2 ± 0.2%; JHH-4, 2.3 ± 0.1%; HuH-1, 32.0 ± 0.1%; HuH-6, 31.5 ± 0.8%; HuH-7, 53.7 ± 2.9%; HLE, 24.9 ± 1.8%; HLF, 8.4 ± 1.7%; PLC/PRF/5, 37.3 ± 2.7%; SK-Hep1, 22.0 ± 2.5%; Hep3B, 45.4 ± 1.9%; HepG2, 59.0 ± 0.9%) was correlated with the indexes of IC_{50} values (correlation coefficient: −0.66534; $R^2 = 0.443$; $p = 0.0129$). The accumulation of polyploid cells is consistent with failed cytokinesis following inhibition of Aurora B kinase activity.

Previously, cellular apoptosis in response to the pan-Aurora kinase inhibitor VX680 was limited in cells expressing wild-type p53 but was enhanced in cells lacking p53 [31]. The p53 point mutations have been reported in four HCC cell lines (HuH-7 at codon 220 Tyr-to-Cys; HLF at codon 244 Gly-to-Ala; HLE and PLC/PRF/5 at codon 249 Arg-to-Ser), and null expression of p53 was reported due to the deletion in the Hep3B cell line, while SK-Hep1 and HepG2 have wild-type p53 [32–34]. There was no significant correlation between the efficacy of AZD1152-HQPA and the p53 status of each cell line in our experiments.

In vitro effects of AZD1152-HQPA on phosphorylation of histone H3 and cell death in human hepatocellular carcinoma cell lines

In the previous studies by Mortlock et al. [35], AZD1152-HQPA is a selective Aurora B kinase inhibitor with more than 1000- to 10,000-fold selectivity for Aurora A kinase and various tyrosine kinases including kinase insert domain receptor (KDR), the Abelson virus kinase (vABL), and epidermal growth factor receptor (EGFR). The inhibition of Aurora B kinase is determined by its specific cellular substrate histone H3 [36]. We investigated whether AZD1152-HQPA was able to inhibit PhH3 in the sensitive SK-Hep1 and Hep3B cells. As shown in Figs. 2 and 3a, AZD1152-HQPA 100 nM yielded a substantial reduction in the level of PhH3. This inhibition of histone H3 phosphorylation was shown to be dose dependent in SK-Hep1 and Hep3B cells treated with AZD1152-HQPA 1–100 nM (Fig. 3B). The cellular apoptosis was confirmed by analysis of Annexin-V binding (Fig. 3C). Cell death rates were measured and were also found be proportional to AZD1152-HQPA dose (Fig. 3D) [21]. These results indicate that inhibition of Aurora B kinase by AZD1152-HQPA can induce cell death in the SK-Hep1 and Hep3B cells *in vitro*. In contrast, the AZD1152-insensitive HLF cells with a low expression of Aurora B kinase (Fig. 1) showed no significant effects on PhH3 and apoptosis compared with SK-Hep1 and Hep3B cells (Figs. 2 and 3).

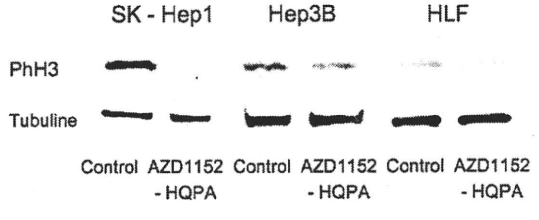

Fig. 2. Effects of AZD1152-hydroxyquinazoline-pyrazol-anilide (AZD1152-HQPA) on phosphorylation of histone H3 in human hepatocellular carcinoma (HCC) cell lines. Western blot analysis of phosphohistone H3 and the control alpha-tubulin in human HCC cell lines after 4-h incubation with AZD1152-HQPA 100 nM or the control DMSO buffer. Cell lines: SK-Hep1 (left), Hep3B (middle), and HLF (right).

In vivo effects of AZD1152 on subcutaneous xenografts of human hepatocellular carcinoma cells

The human HCC cell line SK-Hep1 (AZD1152 IC_{50}: 21.9 nM) is known to be aggressively tumorigenic *in vivo* [37]. To investigate *in vivo* antitumor activity, AZD1152 100 mg/kg per day was administered to nude mice bearing established SK-Hep1 subcutaneous xenografts on 2 consecutive days per week for 2 weeks ($n = 10$). Tumor volumes were measured every other day. As shown in Fig. 4A, significant regression of SK-Hep1 tumors was observed in the group of mice that received AZD1152 compared with control. The mean tumor volumes were substantially decreased by treatment with AZD1152 on day 14 following treatment, and tumor volumes in treated mice were 15.5% of those in control mice (Fig. 4B). None of the AZD1152-treated mice showed signs of wasting or other toxicity relative to control mice. AZD1152 was tolerated at the dose at which antitumor efficacy was observed.

In vivo effects of AZD1152 on orthotopic liver xenografts of human hepatocellular carcinoma cells

A novel orthotopic xenograft model of liver tumors with Matrigel was utilized to explore tumor growth inhibition in situ [25] (Fig. 5A). AZD1152 100 mg/kg was administered to mice bearing SK-Hep1 orthotopic xenografts on 2 consecutive days per week for 2 weeks ($n = 5$). Histological analysis of the liver tumors was conducted within 4 weeks after treatment. Growth of liver tumors was found to be suppressed in all of the mice that had been treated with AZD1152 (Fig. 5B). After drug administration, the mean liver tumor weight in those animals that had received AZD1152 was 10% of that in the control mice (Fig. 5C). Similar growth inhibition was observed in Hep3B orthotopic xenografts by administration of AZD1152 (Fig. 5B and C). In the orthotopic model, mouse survival was significantly enhanced by AZD1152 treatment in comparison with the control ($p < 0.005$; Fig. 5D). These results demonstrate that AZD1152 was able to significantly inhibit *in vivo* growth of a human HCC tumor in the liver microenvironment in mice. All of the host tissues examined, including liver, bone marrow, kidney, intestine, and lung, were histologically normal in all experiments.

Pharmacobiological effects of AZD1152 on orthotopic liver xenografts of human hepatocellular carcinoma cells

The liver xenograft model described above was subjected to histological analysis by immunostaining to investigate the pharmacobiological effects of AZD1152 in the hepatic microenvironment (Fig. 6). Three days after treatment with AZD1152, there was a substantial decrease in PhH3 (Fig. 6E and H) compared with the control (Fig. 6D and G), although after 5 days, PhH3 had recovered (Fig. 6F and I). Staining of tumor samples for apoptotic marker cCasp-3 showed gradually elevating levels following AZD1152 treatment (Fig. 6J–O). The hepatocytes from the host liver were histologically normal at all points following AZD1152 administration (Fig. 6A–C).

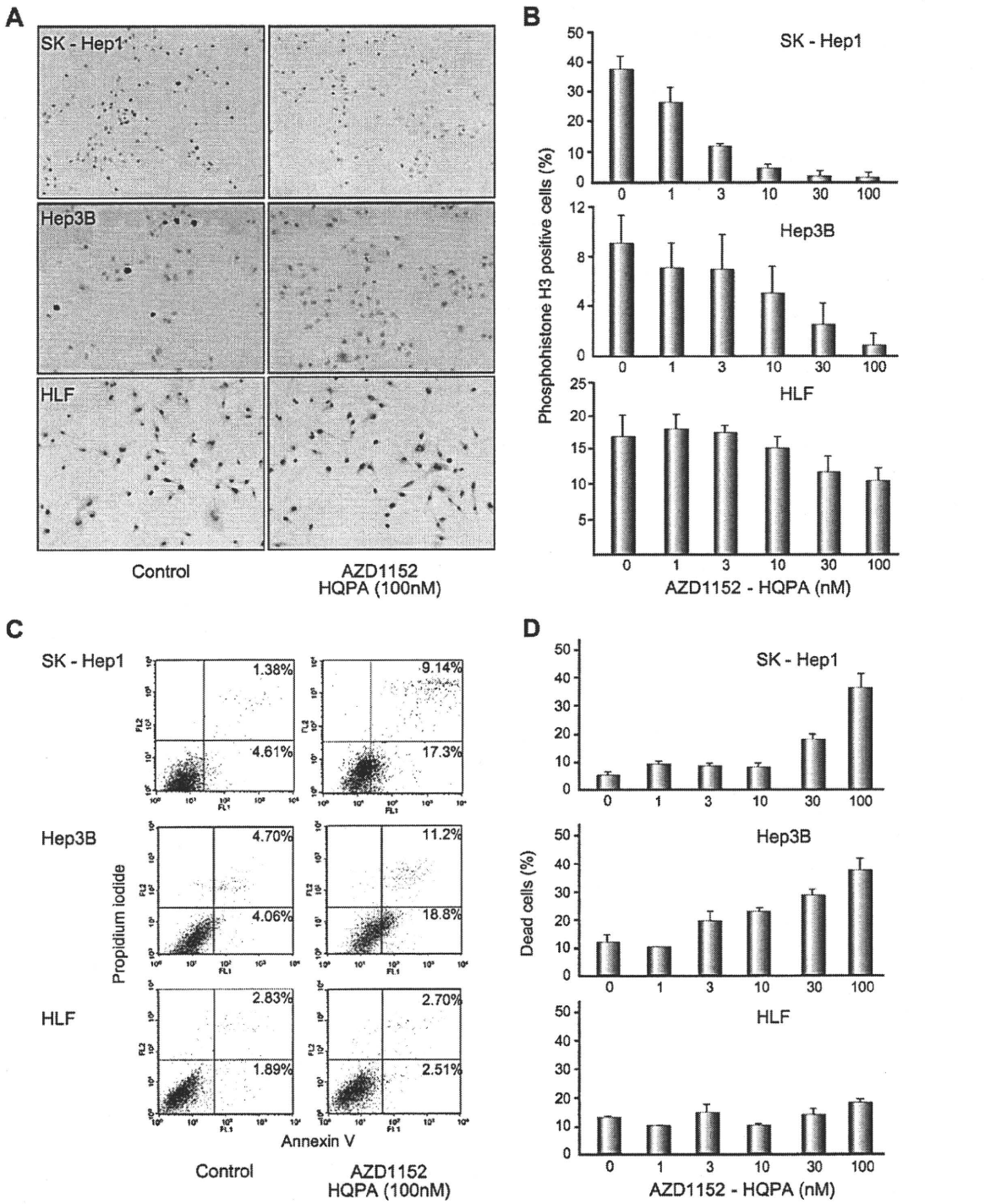

Fig. 3. Dose-dependent effects of AZD1152-hydroxyquinazoline-pyrazol-anilide (AZD1152-HQPA) on phosphorylation of histone H3 and cell death of human hepatocellular carcinoma (HCC) cell lines. (A) Immunocytochemistry of phosphohistone H3 (PhH3) in human HCC cells after 4-h incubation with AZD1152-HQPA 100 nM or the control DMSO buffer. Magnification ×200. Cell lines: SK-Hep1 (upper), Hep3B (middle), and HLF (lower). (B) Dose–response analysis showing percentage of PhH3-positive HCC cells analyzed by immunocytochemistry. Cell lines: SK-Hep1 (upper), Hep3B (middle), and HLF (lower). Columns, PhH3-positive cells (%); vertical bars, standard deviation. (C) AZD1152-HQPA induces apoptosis. SK-Hep1 (upper), Hep3B (middle), and HLF (lower) cells were treated with AZD1152-HQPA for 72 h, and apoptosis was assessed by flowcytometric analysis of cells labeled with Annexin V and propidium iodide. (D) Dose–response analysis showing percentage of nonviable cells in SK-Hep1, Hep3B, and HLF cell samples analyzed using a hemocytometer and trypan blue dye exclusion. Columns, dead cells (%); vertical bars, standard deviation.

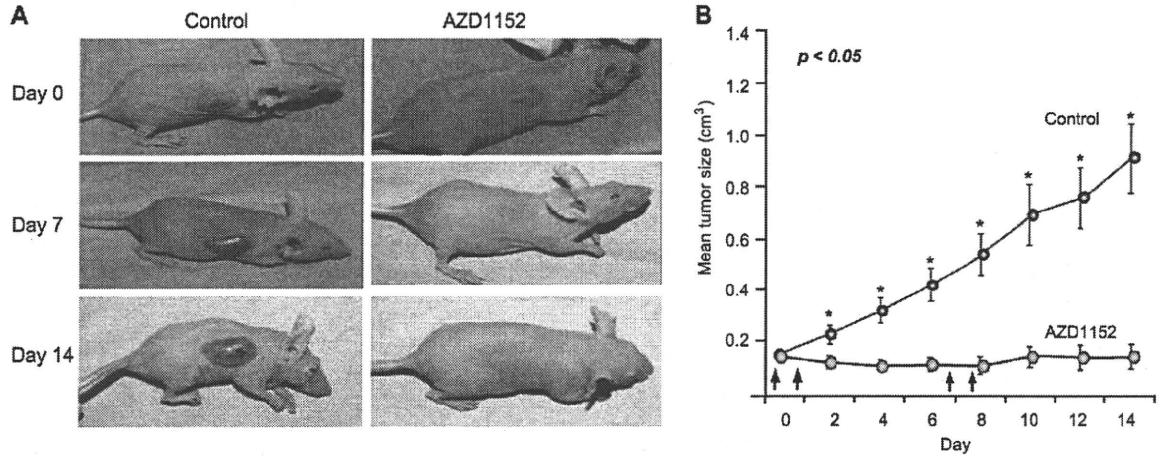

Fig. 4. *In vivo* effects of AZD1152 on human hepatocellular carcinoma (HCC) growth in subcutaneous xenograft models. Established subcutaneous xenografts of SK-Hep1 were treated with intraperitoneal AZD1152 100 mg/kg or the control Tris buffer on 2 consecutive days per week for 2 weeks. (A) Subcutaneous SK-Hep1 tumors in mice on days 0, 7, or 14 following treatment with AZD1152 (right) or the control (left). (B) Tumor volumes were measured and plotted every other day in AZD1152-treated or control mice ($n = 10$). Arrows, timing of administration; vertical bars; standard error. Statistical analysis was done by two-tailed Student t test (*$p < 0.05$).

Discussion

The Aurora family of serine–threonine kinases has recently emerged as a key mitotic regulator required for genome stability [38]. In mammals, the Aurora family consists of three members: Aurora A and B kinases and the less well-characterized Aurora C kinase. Aurora B kinase has been clearly shown to regulate kinetochore function, as it is required for correct chromosome alignment and segregation, spindle-checkpoint function, and cytokinesis. As Aurora kinases are frequently overexpressed in various tumors [39], they have received much attention as potential targets for novel anticancer therapeutics. Treatment with Aurora kinase inhibitors induces the accumulation of cells arrested in a pseudo-G1 state with >4N DNA content or the accumulation of cells with >4N DNA content, the latter population representing cells that exit mitosis and subsequently proceed through S phase in the absence of cell division [31]. Continued proliferation in the presence of aberrant mitosis and failed cytokinesis presumably gives rise to cells with higher DNA content due to an increase of the cell diameter, resulting in apoptosis [17,18,40,41]. The defective cytokinesis, as well as the inhibition of PhH3 by Aurora kinase inhibitors, suggests that the cellular effects of Aurora kinase inhibitors might be largely mediated by the disruption of Aurora B kinase function [18]. AZD1152 is a selective inhibitor of Aurora kinase with specificity for Aurora B kinase. AZD1152 has the potential to be efficacious in multiple tumor types and is currently undergoing phase 1 clinical evaluation as a treatment for a range of malignancies [20,21].

We have previously identified Aurora B kinase as the only independent predictor for the aggressive recurrence of human HCC [10]. In our present study, AZD1152-HQPA substantially reduced *in vitro* proliferation in a variety of human HCC cell lines. The extent of proliferation inhibition was correlated with Aurora B kinase expression levels (Fig. 1). As shown in Fig. 1C, significant DNA fragmentation in the form of a sub-G1 peak could not be detected after 24 h of treatment with AZD1152-HQPA, which is in line with data reported by Wilkinson et al. [20]. This inability to detect a sub-G1 population after AZD1152-HQPA treatment may result because inhibition of Aurora B kinase induces polyploidy before apoptosis, in which case DNA fragmentation will occur in the >4N population, making it difficult to detect a sub-G1 population.

Treatment with AZD1152-HQPA also led to inhibition of PhH3 as well as failure of tumor cell division, and ultimately induced death of human HCC cells (Figs. 2 and 3). *In vivo* administration of AZD1152 suppressed the growth of human HCC tumors in established subcutaneous xenografts (Fig. 4). Although subcutaneous xenograft models have the benefits of easy visualization and monitoring of tumor growth, the biological response to therapeutic agents in the natural microenvironment of the tumor should be analyzed using orthotopic xenograft models [30,42]. In this study, a novel model of intrahepatic inoculation with Matrigel was utilized to closely mimic HCC tumors in humans [24]. As shown in Fig. 5, AZD1152 inhibited *in vivo* growth of established liver tumors and increased survival in this model. Furthermore, pharmacobiological studies of AZD1152 confirmed *in vivo* suppression of PhH3 and induction of cellular apoptosis of human HCC (Fig. 6). AZD1152 was well tolerated at the dose required to elicit a potent and durable antitumor effect in mice. According to the previous report by Wilkinson et al. [20], mice were almost resistant to myelosuppression after AZD1152 treatment; the authors could not find any reductions in bone marrow nucleated cells at the end of the dosing period. In rats, there was a myelosuppressive effect of AZD1152 that was associated with a reduction in bone marrow nucleated cells to 34% of that seen in the controls at the end of the 48-h dosing period; however, the bone marrow nucleated cell content rapidly recovered such that it was 104.8% of control at the end of the study period. Although the phase 1 studies on the side effects of AZD1152 have not yet been reported in detail, humans might be more sensitive to the myelosuppressive effects compared to the experimental rodents. Further study should be required for clinical application to HCC patients, especially those with cirrhosis.

Clinical evidence exists indicating a significant relationship between Aurora B kinase expression and the aggressive progression of HCC [10], and our preclinical studies indicated that

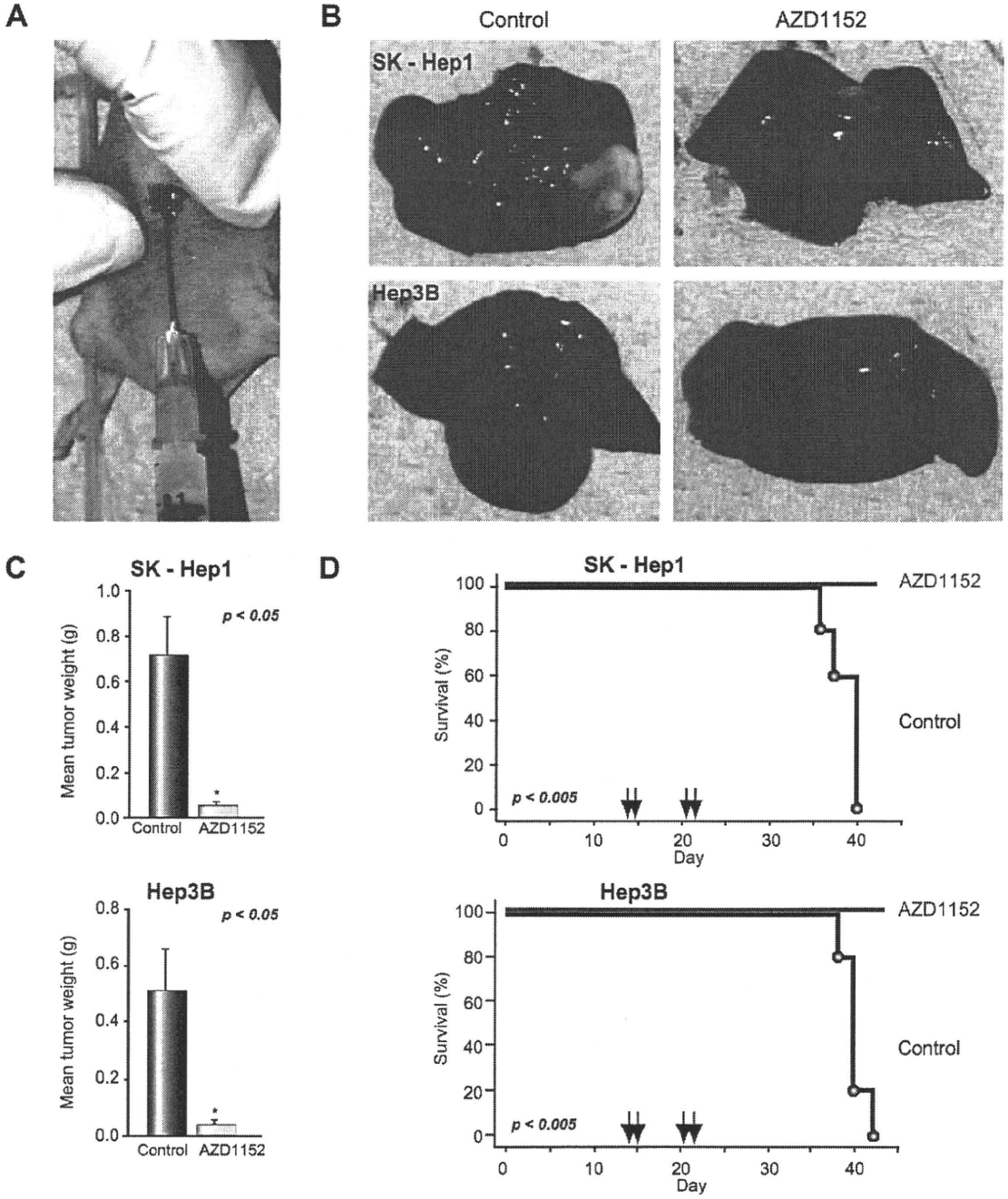

Fig. 5. *In vivo* effects of AZD1152 on human hepatocellular carcinoma (HCC) growth in orthotopic xenograft models. (A) Schematic representation of generation of orthotopic xenografts. A small transverse incision was made below the sternum to expose the liver, and 2.5×10^6 cells with Matrigel were then slowly injected at a 30° angle into the upper left lobe of the liver using a 28-gauge needle. After 14 days, the mice were treated intraperitoneally with AZD1152 100 mg/kg or the control Tris buffer on 2 consecutive days per week for 2 weeks. (B) The liver tumor in mice within 4 weeks after administration of AZD1152 (light) and the control (right). Cell lines: SK-Hep1 (upper) and Hep3B (lower). (C) Liver tumor weight was analyzed within 4 weeks after administration of AZD1152 or the control ($n = 5$). SK-Hep1 (upper), and Hep3B (lower). Vertical bars, standard error. Statistical analysis was done by two-tailed Student t test ($^*p < 0.05$). (D) Results are expressed in terms of percent survival in experiment time. Arrows, timing of administration. Statistical differences were analyzed by Mantel–Cox log-rank test ($p < 0.005$).

AZD1152, a specific inhibitor of Aurora B kinase, is a promising novel therapeutic approach for the treatment of human HCC. Urgent studies and clinical trials of AZD1152 will confirm its role in the treatment of HCC.

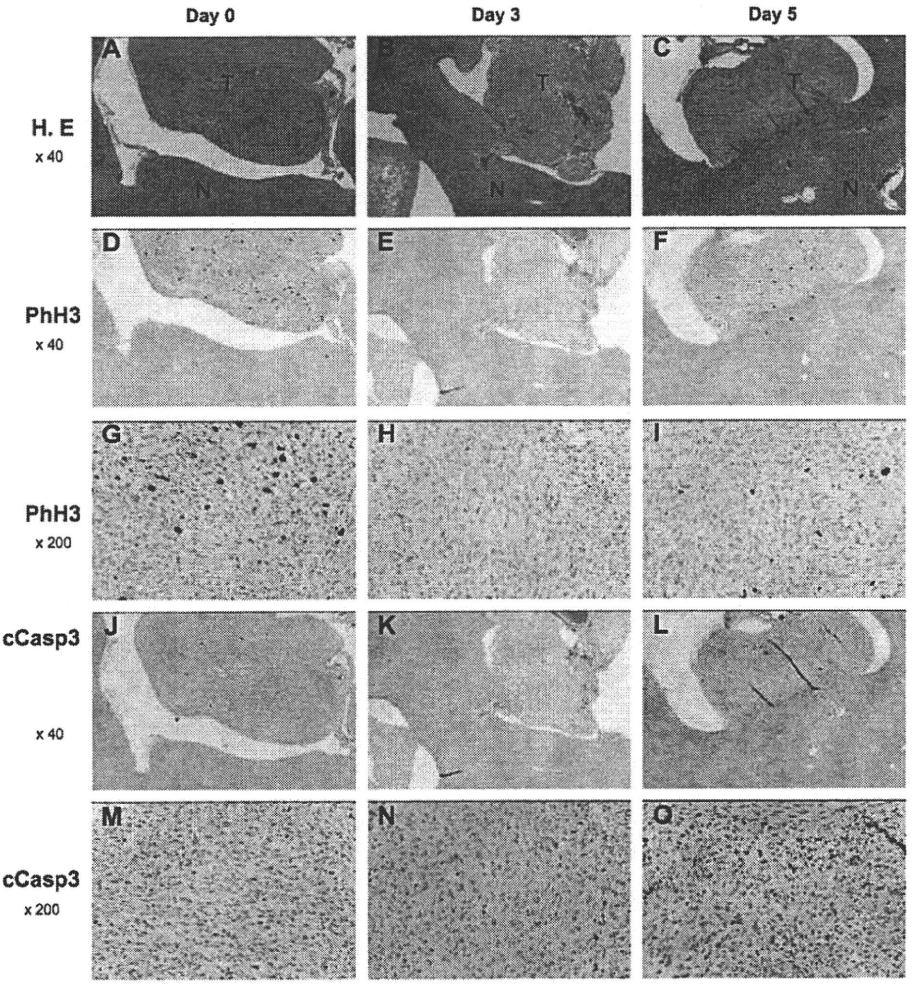

Fig. 6. Pharmacobiological analysis of orthotopic xenograft models. Established orthotopic xenografts of human SK-Hep1 hepatocellular carcinoma (HCC) cells were treated intraperitoneally with AZD1152 100 mg/kg on 2 consecutive days. Mice were sacrificed humanely on day 0 prior to treatment and on days 3 and 5 after the first administration of AZD1152 (left, middle and right, respectively). (A–C) Transverse sections of liver tumor (T) or host normal liver (N) were stained with hematoxylin and eosin (HE; magnification ×40). The same sections were analyzed for expression of phosphohistone H3 (PhH3): (D–F) magnification ×40 and (G–I) magnification ×200. The same sections were also analyzed for the apoptotic marker of cleaved caspase-3 (cCasp-3): (J–L) magnification ×40 and (M–O) magnification ×200.

Acknowledgments

The authors who have taken part in this study declared that they do not have anything to disclose regarding funding from industries or conflict of interest with respect to this manuscript.

This research was supported by the Ministry of Education, Science and Culture, Grant-in-Aid for Scientific Research.

We thank AstraZeneca for kindly providing us with AZD1152 and AZD1152-HQPA for experimental studies. We also thank Drs. Robert Wilkinson, Elizabeth Anderson (AstraZeneca) for helpful discussion, Sarah Mason (Mudskipper Bioscience) for editorial assistance, Kaoru Mogushi for statistical analysis, Akimoto Nimura for technical advice regarding flow cytometry, and Ayumi Shioya for technical assistance.

References

[1] Farazi PA, DePinho RA. Hepatocellular carcinoma pathogenesis: from genes to environment. Nat Rev Cancer 2006;6:674–687.

[2] Ince N, Wands JR. The increasing incidence of hepatocellular carcinoma. N Engl J Med 1999;340:798–799.

[3] Arii S, Yamaoka Y, Futagawa S, Inoue K, Kobayashi K, Kojiro M, et al. Results of surgical and nonsurgical treatment for small-sized hepatocellular carcinomas: a retrospective and nationwide survey in Japan. The Liver Cancer Study Group of Japan. Hepatology 2000;32:1224–1229.

[4] Sherman M. Recurrence of hepatocellular carcinoma. N Engl J Med 2008;359:2045–2047.

[5] Llovet JM, Burroughs A, Bruix J. Hepatocellular carcinoma. Lancet 2003;362:1907–1917.

[6] Llovet JM, Ricci S, Mazzaferro V, Hilgard P, Gane E, Blanc JF, et al. Sorafenib in advanced hepatocellular carcinoma. N Engl J Med 2008;359:378–390.

[7] Zhu AX. Development of sorafenib and other molecularly targeted agents in hepatocellular carcinoma. Cancer 2008;112:250–259.
[8] Tanaka S, Sugimachi K, Maehara S, Harimoto N, Shirabe K, Wands JR. Oncogenic signal transduction and therapeutic strategy for hepatocellular carcinoma. Surgery 2002;131:S142–S147.
[9] Tanaka S, Noguchi N, Ochiai T, Kudo A, Nakamura N, Ito K, et al. Outcomes and recurrence of initially resectable hepatocellular carcinoma meeting Milan criteria: rationale for partial hepatectomy as first strategy. J Am Coll Surg 2007;204:1–6.
[10] Tanaka S, Arii S, Yasen M, Mogushi K, Su NT, Zhao C, et al. Aurora kinase B is a predictive factor for the aggressive recurrence of hepatocellular carcinoma after curative hepatectomy. Br J Surg 2008;95:611–619.
[11] Lee EC, Frolov A, Li R, Ayala G, Greenberg NM. Targeting Aurora kinases for the treatment of prostate cancer. Cancer Res 2006;66:4996–5002.
[12] Bischoff JR, Anderson L, Zhu Y, Mossie K, Ng L, Souza B, et al. A homologue of Drosophila aurora kinase is oncogenic and amplified in human colorectal cancers. EMBO J 1998;17:3052–3065.
[13] Li D, Zhu J, Firozi PF, Abbruzzese JL, Evans DB, Cleary K, et al. Overexpression of oncogenic STK15/BTAK/Aurora A kinase in human pancreatic cancer. Clin Cancer Res 2003;9:991–997.
[14] Smith SL, Bowers NL, Betticher DC, Gautschi O, Ratschiller D, Hoban PR, et al. Overexpression of aurora B kinase (AURKB) in primary non-small cell lung carcinoma is frequent, generally driven from one allele, and correlates with the level of genetic instability. Br J Cancer 2005;93: 719–729.
[15] Tanaka T, Kimura M, Matsunaga K, Fukada D, Mori H, Okano Y. Centrosomal kinase AIK1 is overexpressed in invasive ductal carcinoma of the breast. Cancer Res 1999;59:2041–2044.
[16] Sorrentino R, Libertini S, Pallante PL, Troncone G, Palombini L, Bavetsias V, et al. Aurora B overexpression associates with the thyroid carcinoma undifferentiated phenotype and is required for thyroid carcinoma cell proliferation. J Clin Endocrinol Metab 2005;90:928–935.
[17] Gautschi O, Heighway J, Mack PC, Purnell PR, Lara Jr PN, Gandara DR. Aurora kinases as anticancer drug targets. Clin Cancer Res 2008;14:1639–1648.
[18] Keen N, Taylor S. Aurora-kinase inhibitors as anticancer agents. Nat Rev Cancer 2004;4:927–936.
[19] Macarulla T, Ramos FJ, Tabernero J. Aurora kinase family: a new target for anticancer drug. Recent Patents Anticancer Drug Discov 2008;3:114–122.
[20] Wilkinson RW, Odedra R, Heaton SP, Wedge SR, Keen NJ, Crafter C, et al. AZD1152, a selective inhibitor of Aurora B kinase, inhibits human tumor xenograft growth by inducing apoptosis. Clin Cancer Res 2007;13:3682–3688.
[21] Yang J, Ikezoe T, Nishioka C, Tasaka T, Taniguchi A, Kuwayama Y, et al. AZD1152, a novel and selective aurora B kinase inhibitor, induces growth arrest, apoptosis, and sensitization for tubulin depolymerizing agent or topoisomerase II inhibitor in human acute leukemia cells in vitro and *in vivo*. Blood 2007;110:2034–2040.
[22] Hoshida Y, Villanueva A, Kobayashi M, Peix J, Chiang DY, Camargo A, et al. Gene expression in fixed tissues and outcome in hepatocellular carcinoma. N Engl J Med 2008;359:1995–2004.
[23] Tredan O, Galmarini CM, Patel K, Tannock IF. Drug resistance and the solid tumor microenvironment. J Natl Cancer Inst 2007;99:1441–1454.
[24] Han C, Wu T. Cyclooxygenase-2-derived prostaglandin E2 promotes human cholangiocarcinoma cell growth and invasion through EP1 receptor-mediated activation of the epidermal growth factor receptor and Akt. J Biol Chem 2005;280:24053–24063.
[25] Lu YS, Kashida Y, Kulp SK, Wang YC, Wang D, Hung JH, et al. Efficacy of a novel histone deacetylase inhibitor in murine models of hepatocellular carcinoma. Hepatology 2007;46:1119–1130.
[26] Harrington EA, Bebbington D, Moore J, Rasmussen RK, Ajose-Adeogun AO, Nakayama T, et al. VX-680, a potent and selective small-molecule inhibitor of the Aurora kinases, suppresses tumor growth in vivo. Nat Med 2004;10:262–267.
[27] Soncini C, Carpinelli P, Gianellini L, Fancelli D, Vianello P, Rusconi L, et al. PHA-680632, a novel Aurora kinase inhibitor with potent antitumoral activity. Clin Cancer Res 2006;12:4080–4089.
[28] Tanaka S, Pero SC, Taguchi K, Shimada M, Mori M, Krag DN, et al. Specific peptide ligand for Grb7 signal transduction protein and pancreatic cancer metastasis. J Natl Cancer Inst 2006;98:491–498.
[29] Tanaka S, Sugimachi K, Yamashita Yi Y, Ohga T, Shirabe K, Shimada M, et al. Tie2 vascular endothelial receptor expression and function in hepatocellular carcinoma. Hepatology 2002;35:861–867.
[30] Raskopf E, Dzienisowicz C, Hilbert T, Rabe C, Leifeld L, Wernert N, et al. Effective angiostatic treatment in a murine metastatic and orthotopic hepatoma model. Hepatology 2005;41:1233–1240.
[31] Gizatullin F, Yao Y, Kung V, Harding MW, Loda M, Shapiro GI. The Aurora kinase inhibitor VX680 induces endoreduplication and apoptosis preferentially in cells compromised p53-dependent postmitotic checkpoint function. Cancer Res 2006;66:7668–7677.
[32] Bressac B, Galvin KM, Liang TJ, Isselbacher KJ, Wands JR, Ozturk M. Abnormal structure and expression of p53 gene in human hepatocellular carcinoma. Proc Natl Acad Sci USA 1990;87:1973–1977.
[33] Hsu IC, Tokiwa T, Bennett W, Metcalf RA, Welsh JA, Sun T, et al. P53 gene mutation and integrated hepatitis B viral DNA sequences in human liver cancer cell lines. Carcinogenesis (Lond.) 1993;14:987–992.
[34] Tanaka S, Toh Y, Adachi E, Matsumata T, Mori R, Sugimachi K. Tumor progression in hepatocellular carcinoma may be mediated by p53 mutation. Cancer Res 1993;53:2884–2887.
[35] Mortlock AA, Foote KM, Heron NM, Jung FH, Pasquet G, Lohmann JJ, et al. Discovery, synthesis, and in vivo activity of a new class of pyrazoloquinazolines as selective inhibitors of aurora B kinase. J Med Chem 2007;50:2213–2224.
[36] Hirota T, Lipp JJ, Toh BH, Peters JM. Histone H3 serine 10 phosphorylation by Aurora B causes HP1 dissociation from heterochromatin. Nature 2005;438:1176–1180.
[37] Maret A, Galy B, Arnaud E, Bayard F, Prats H. Inhibition of fibroblast growth factor 2 expression by antisense RNA induced a loss of the transformed phenotype in a human hepatoma cell line. Cancer Res 1995;55:5075–5079.
[38] Giet R, Petretti C, Prigent C. Aurora kinases, aneuploidy and cancer, a coincidence or a real link? Trends Cell Biol 2005;15:241–250.
[39] Hontz AE, Li SA, Lingle WL, Negron V, Bruzek A, Salisbury JL, et al. Aurora A and B overexpression and centrosome amplification in early estrogen-induced tumor foci in the Syrian hamster kidney: implications for chromosomal instability, aneuploidy, and neoplasia. Cancer Res 2007;67:2957–2963.
[40] Warner SL, Bearss DJ, Han H, Von Hoff DD. Targeting Aurora-2 kinase in cancer. Mol Cancer Ther 2003;2:589–595.
[41] Carmena M, Earnshaw WC. The cellular geography of aurora kinases. Nat Rev Mol Cell Biol 2003;4:842–854.
[42] Yao X, Hu JF, Daniels M, Yien H, Lu H, Sharan H, et al. A novel orthotopic tumor model to study growth factors and oncogenes in hepatocarcinogenesis. Clin Cancer Res 2003;9:2719–2726.

Gene Expression Signature of the Gross Morphology in Hepatocellular Carcinoma

Ayano Murakata, MD, Shinji Tanaka, MD, PhD, FACS*, Kaoru Mogushi, PhD†, Mahmut Yasen, MD, PhD†, Norio Noguchi, MD, PhD*, Takumi Irie, MD, PhD*, Atsushi Kudo, MD, PhD*, Noriaki Nakamura, MD, PhD*, Hiroshi Tanaka, PhD†, and Shigeki Arii, MD, PhD**

Objective: To evaluate the gene expression signature of hepatocellular carcinoma (HCC) in relation to the gross morphology.

Background: Eggel's nodular type of HCC is morphologically subclassified into the single nodular (SN) type, the single nodular type with extranodular growth (SNEG), and the confluent multinodular (CM) type, but their biomolecular differences remain unclear.

Methods: The clinicopathological characteristics and genome-wide gene expressions were analyzed in 275 patients with nodular-type HCC (124 SN-type, 91 SNEG-type, and 60 CM-type) who received curative hepatectomy.

Results: Significantly poor prognosis was recognized in CM types in overall survival ($P = 0.0020$) and recurrence-free survival ($P = 0.0066$). Analysis of the genome-wide expression patterns revealed significant difference of CM-type HCC from either SN- or SNEG-type HCC. In particular, a stem cell marker EpCAM was dominantly expressed in CM-type HCC. Immunohistochemical studies confirmed the specific expression of EpCAM in HCC cancer cells of CM type. In multivariate analysis, the gross morphology of CM type was significantly associated with EpCAM expression ($P = 0.0092$), α-fetoprotein ($P = 0.0424$), "lens culinaris agglutinin-reactive fraction of α-fetoprotein" level ($P = 0.0288$), and the portal vein invasion ($P = 0.0150$). Furthermore, EpCAM was predictive for poor prognosis in overall and recurrence-free survivals of patients with CM-type HCC ($P = 0.0082$ and $P = 0.0043$, respectively).

Conclusion: Our studies suggest that the distinct signature of gene expression is closely related to morphological progression in HCC. Especially, EpCAM might play a critical role in the aggressiveness of CM-type HCC.

(*Ann Surg* 2011;253:94–100)

Tumor morphologies have been identified to associate with their malignant properties[1,2] and the differences of gene expression pattern in cancers.[3,4] Analysis of the preoperative morphology might be apparently predictive for the invasive, metastatic, and/or even recurrent potentials after cancer treatment.[1,2,5] Hepatocellular carcinoma (HCC) is known to demonstrate various morphological appearances.[6] In 1901, Eggel[7] established a classical gross classification of HCC morphology into nodular, massive, and diffuse types on the basis of the autopsy data. As modifications for the surgically resectable HCC by Kanai et al,[8] the nodular type has been subclassified into 3 categories of gross appearance: single nodular (SN) type, single nodular type with extranodular growth (SNEG), and confluent multinodular (CM) type, in accordance with the clinicopathological features.[9,10] Indeed, there are many studies indicating that the SN type showed better prognosis but more malignant potentials were recognized in the CM type of HCC.[11–14] Although this gross classification is widely used as one of the prognostic factors after HCC treatment not only for surgical resection[9] but also for chemoembolization[15,16] and ablation therapy,[17] the molecular backgrounds and differences have not been clarified yet.

Genome-wide transcriptional analysis by microarray offers a systematic approach to unfold comprehensive information regarding the gene expression profiles.[18,19] Furthermore, such studies should potentially lead not only to identification of unique biomarkers[20] but also to development of novel molecular targets for therapy.[21] We have previously analyzed gene expression of lethal recurrence of HCC[22] and identified a novel biomarker and targeting molecule.[23] Our present study aimed at seeking gene signatures and biomarkers associated with the morphological appearance of nodular-type HCC. This is the first report of the genome-wide expression profile of HCC morphology as generated from microarray study. Consequently, the molecular features and potential targets for therapy were found with special emphasis on the morphological progression in HCC.

MATERIALS AND METHODS

Subjects and Tissue Samples

Between April 2000 and October 2008, 275 patients with nodular-type HCC underwent curative hepatectomy at the Tokyo Medical and Dental University Hospital. Written informed consent was obtained from each subject, and study procedures were approved by the institutional review board. Preoperative evaluations, including tumor markers α-fetoprotein (AFP), lens culinaris agglutinin-reactive fraction of AFP (AFP-L3), and protein induced by vitamin K absence or antagonists-II (PIVKA-II), were essentially described elsewhere.[22] According to the General Rules for the Clinical and Pathological Study of Primary Liver Cancer by Liver Cancer Study Group of Japan,[24] 275 cases were pathologically subclassified into 124 SN-type, 91 SNEG-type, and 60 CM-type HCCs. The largest area of the lesion was evaluated to determine the gross type. When more than 1 grow type were present, the predominant type (the one with a larger volume) was recorded in this study. The diagnosis was evaluated by 3 independent pathologists. Resected tissues were further analyzed as described previously.[22]

Microarray Analysis of Gene Expression

The tissue preparation was essentially compliant with the General Rules for the Clinical and Pathological Study of Primary Liver Cancer.[24] For the gene expression analysis, at least 3 sections of the largest nodule were used from the largest cross section of the main tumor. Total RNA was extracted from HCC specimens by using an RNeasy kit (Qiagen, Hilden, Germany). The integrity of the obtained RNA (RNA integrity number > 5.0) was confirmed using an Agilent 2100 BioAnalyzer (Agilent Technologies, Palo Alto, Calif). For further analysis of gene expression, 129 samples, 62 SN-type,

From the *Department of Hepato-Biliary-Pancreatic Surgery and †Information Center for Medical Sciences, Tokyo Medical and Dental University, Tokyo, Japan.

No conflicts of interest exist.

Reprints: Shinji Tanaka, MD, PhD, FACS, Department of Hepato-Biliary-Pancreatic Surgery, Tokyo Medical and Dental University, Graduate School of Medicine, 1-5-45 Yushima, Bunkyo-ku, Tokyo 113-8519, Japan. E-mail: shinji.msrg@tmd.ac.jp.

ISSN: 0003-4932/11/25301-0094
DOI: 10.1097/SLA.0b013e3181f9bc00

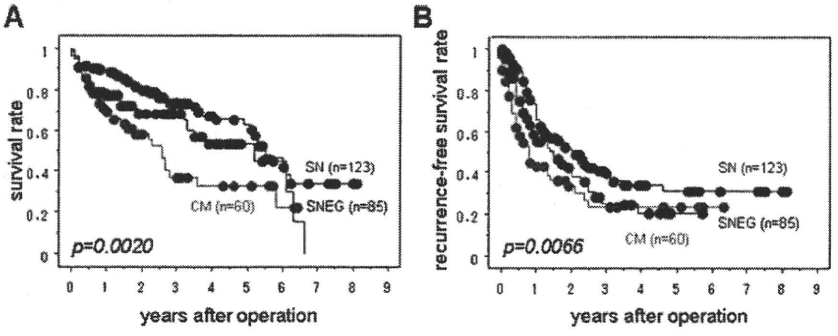

FIGURE 1. Postoperative prognosis of patients with HCC according to the gross morphology of SN, SNEG, and CM types. (A) Overall survival curves and (B) recurrence-free survival curves. Log-rank test demonstrated statistically significant differences in overall and recurrence-free survival rates ($P = 0.0020$ and $P = 0.0066$, respectively).

TABLE 1. The Differentially Expressed Genes in CM-Type HCC by Ranking of the Fold Change (Top 20)

Symbol	Title	*P*	Fold Change
EpCAM	Epithelial cell adhesion molecule (TACSTD1)	1.84E-03	3.43
SLC39A4	Solute carrier family 39 (zinc transporter), member 4	3.24E-05	2.65
CTHRC1	Collagen triple helix repeat containing 1	3.14E-03	2.62
ELOVL7	ELOVL family member 7	8.04E-03	2.37
EPPK1	Epiplakin 1	3.48E-03	2.15
ZNF83	Zinc finger protein 83	1.21E-04	2.14
FOXQ1	Forkhead box Q1	8.49E-03	2.14
NT5DC2	5′-nucleotidase domain containing 2	4.55E-05	2.13
FGFR2	Fibroblast growth factor receptor 2	9.46E-03	2.10
ZNF331	Zinc finger protein 331	1.17E-03	2.03
GTSE1	G-2 and S-phase expressed 1	4.81E-05	1.99
TMED3	Transmembrane emp24 protein transport domain containing 3	4.07E-03	1.99
GLRB	Glycine receptor, β	5.23E-05	1.93
B3GNT5	β-1,3-*N*-acetylglucosaminyltransferase 5	5.14E-03	1.91
—	CDNA FLJ30069 fis, clone ASTRO1000096	3.48E-03	1.89
FADS1/3	Fatty acid desaturase 1/fatty acid desaturase 3	4.58E-03	1.89
DUSP9	Dual specificity phosphatase 9	2.23E-03	1.88
RAP1GAP	RAP1 GTPase activating protein	9.77E-04	1.80
PNMA6A	Paraneoplastic antigen like 6A	6.95E-04	1.80
FAM72A	Gastric cancer upregulated-2/family with sequence similarity 72 A	1.52E-03	1.79

36 SNEG-type, and 31 CM-type HCCs, were available.#12288; Contaminant DNA was removed by digestion with RNase-free DNase (Qiagen). Using 2 μg of total RNA, cRNA was prepared using 1-cycle target labeling and control reagents kit (Affymetrix, Santa Clara, Calif). Hybridization and signal detection of HG-U133 Plus 2.0 arrays (Affymetrix) were performed as per the manufacturer's instructions. Microarray data sets were normalized using a robust multiarray average method under R 2.9.0 statistical software together with a BioConductor package, as previously described.[22]

Profiling Analyses Using Microarray Data

Fold-change (FC) values were calculated using ratios of geometric means of gene expression levels between subtypes for each of the 54,613 probes on the HG-U133 Plus 2.0 array. Genes differently expressed among SN, SNEG, and CM were evaluated by the Kruskal-Wallis test. False discovery rate (FDR) was used to correct multiple comparisons with microarray data analysis. FDR < 30% (equivalent to $P < 0.00056$ in this case) was used as the selection criteria. Using selected probe sets, principal component (PC) analysis was performed to investigate the analogy of gene expression in relation to the 3 gross morphology patterns.[25] Hierarchical clustering with selected genes was also performed on R software by using the Pearson correlation coefficient as a similarity index and a complete linkage method for agglomeration. For visualization, expression intensities were standardized by *z* scores (mean = 0 and variance = 1) for each probe set. In addition, the gene expression profiles between 2 groups were analyzed by Mann-Whitney *U* test. The *P*-value distributions were represented by the number of probe sets with an interval of 0.05 *P*-value, as essentially described by Boersma et al.[26]

Immunohistochemical Analysis

To validate the protein expression, immunohistochemical analysis was performed on tissue sections. For the tissue analysis, 262 samples, 117 SN-type, 88 SNEG-type, and 57 CM-type HCCs, were available.#12288; Stained using anti-EpCAM (extracellular domain) monoclonal antibody (clone VU-1D9; AbD Serotec, Oxford, United Kingdom) at 1:100 dilutions with PBS containing 1% bovine serum albumin (Sigma), followed by reactions in an automated immunostainer (Ventana XT System) using and a standard DAB detection kit (Ventana). Tissue samples with any staining in the HCC cancer cells were diagnosed as positive, and the others were diagnosed as negative immunohistochemically. The immunostaining was evaluated under a light microscope by 2 independent investigators.

TABLE 2. Univariate Analysis of Clinicopathologic Features According to the Gross Morphology of HCC

	SN (n = 124)	SNEG (n = 91)	CM (n = 60)	*P*
Age, y	66.5 ± 0.8	66.8 ± 0.9	63.9 ± 1.5	0.14
Sex				0.65
Male	93	73	47	
Female	31	18	13	
Background liver				0.32
Normal liver	5	7	3	
Chronic hepatitis	52	47	23	
Liver cirrhosis	67	36	34	
Albumin, g/dL	3.9 ± 0.1	3.7 ± 0.1	3.8 ± 0.1	0.15
Total bilirubin, mg/dL	0.9 ± 0.1	0.9 ± 0.1	0.9 ± 0.1	0.80
PT%	84.8 ± 1.2	83.7 ± 1.2	83.4 ± 1.6	0.71
AFP, ng/mL	686 ± 265	4204 ± 2007	8536 ± 3541	**0.04** (SN vs SNEG)
				0.0019 (SN vs CM)
				0.26 (SNEG vs CM)
AFP-L3, %	11.2 ± 1.8	16.4 ± 2.9	29.8 ± 4.7	0.11 (SN vs SNEG)
				<0.0001 (SN vs CM)
				0.012 (SNEG vs CM)
PIVKAII, mAU/mL	1714 ± 478	6987 ± 2709	14,865 ± 8573	0.05
Tumor size, cm	3.7 ± 0.2	5.1 ± 0.3	5.4 ± 0.5	**0.0001** (SN vs SNEG)
				0.0002 (SN vs CM)
				0.62 (SNEG vs CM)
Tumor differentiation				0.13
Well	21	12	4	
Moderately	64	45	23	
Poorly	34	32	27	
Portal vein invasion				**<0.0001** (SN vs SNEG)
Positive	21	39	39	**<0.0001** (SN vs CM)
Negative	103	52	21	**0.008** (SNEG vs CM)
Hepatic vein invasion				**0.0002** (SN vs SNEG)
Positive	4	18	16	**<0.0001** (SN vs CM)
Negative	120	73	44	0.32 (SNEG vs CM)
Tumor-node-metastatis stage				
I	22	4	4	
II	63	26	10	**<0.0001** (SN vs SNEG)
III	35	34	22	**<0.0001** (SN vs CM)
IVA	4	26	17	0.59 (SNEG vs CM)
IVB	0	1	3	
Surgical procedure				**0.0068** (SN vs SNEG)
Anatomical	72	69	39	0.3673 (SN vs CM)
Nonanatomical	52	22	21	0.1492 (SNEG vs CM)
EpCAM protein				0.5725 (SN vs SNEG)
Positive	28	25	29	**0.0007** (SN vs CM)
Negative	89	63	28	**0.0105** (SNEG vs CM)

The significance of p values in bold.

Statistical Analysis

All quantitative variables in comparison of the 3 groups were assessed by analysis of variance and Student *t* test with the Bonferroni adjustment for multiple comparisons. Chi-square test was used to compare the qualitative variables. After the univariate analysis, the significant variables were further used for the multivariate analysis according to the logistic regression model. Survival curves were constructed using the Kaplan-Meier method and compared with the log-rank test. Cox's proportional-hazards model was used to evaluate the contribution of variables. *P* values of < 0.05 were considered to have statistical significance.

RESULTS

Postoperative Outcomes of Patients With HCC According to the Gross Morphology

The gross morphology of HCC has been reported to relate closely to its malignant properties.[6,9] We first assessed the

postoperative prognosis of 275 patients with nodular-type HCC composed of 124 SN-type, 91 SNEG-type, and 60 CM-type cases. As shown in Figure 1, the gross morphology was significantly associated with the overall survivals and recurrence-free survivals of patients after curative hepatectomy ($P = 0.0020$ and $P = 0.0066$, respectively). The overall and recurrence-free survivals of patients with CM-type HCC were significantly poorer than those with SN type ($P = 0.0004$ and $P = 0.0020$, respectively), but the difference was marginal compared with SNEG type ($P = 0.0971$ and $P = 0.1776$, respectively). Relatively poor prognosis of HCC patients with SNEG type was recognized in comparison with those with SN type ($P = 0.0503$ and $P = 0.0521$, respectively).

Gene Signature of HCC According to the Gross Morphology

Next, genome-wide expression of genes was analyzed using cDNA microarray, followed by evaluation by the Kruskal-Wallis test to compare among the 3 categories. FDR < 30% was utilized as the selection criteria, and then selected 1022 probe sets were further evaluated for PC analysis and hierarchical clustering. Using the selected probe sets, PC analysis was performed to investigate the analogy of gene expression patterns in relation to 3 categories of the gross morphology.[25] Figure 2A demonstrates the scatter spot graphics of the first PC, the second PC, and the third PC. Although SN (black) and SNEG cases (blue) tended to cluster together, most of CM cases (red) were clearly divided from the SN/SNEG cluster. Analysis of hierarchical clustering[22] also showed the distinct pattern of the gene expression in CM cases compared with SN and SNEG cases (Fig. 2B). In addition, based on Mann-Whitney U test to compare between the 2 categories, the P-value distributions were analyzed as described by Boersma et al.[26] Figure 2C demonstrates a significant enrichment of the differentially expressed genes between CM and either SN or SNEG, but not significance between SN and SNEG. The gene signatures of CM-type HCC proved a distinct pattern of expression compared with those of either SN- or SNEG-type HCC.

EpCAM; Specific Expression in CM-type HCC With Clinical Significance

To identify the differentially expressed genes in CM type compared with SN and SNEG types, probe sets satisfied with both $P <$ 0.01 by Mann-Whitney U test and FC > 2.0 were further evaluated. As displayed in Table 1 in order of the FC values, a stem cell marker EpCAM (epithelial cell adhesion molecule) was significantly overexpressed in the CM-type HCC. Immunohistochemical validation of EpCAM protein was then performed using 262 tissue samples of HCC. EpCAM protein was mainly distributed on the cellular membrane in HCC cancer cells of 82 samples (31.3%), but not in those of the remaining 180 samples (68.7%), as represented in Figure 3. Substantially, the immunostaining revealed that EpCAM protein was expressed dominantly in 29 (50.9%) of 57 CM-type HCCs, but only in 28 (23.9%) of the 117 SN types and 25 (28.4%) of the 88 SNEG types ($P = 0.0007$; SN vs CM, $P = 0.0105$; SNEG vs CM).

Univariate analysis for the gross morphology of HCC determined the expression of EpCAM protein, serum level of AFP, AFP-L3, tumor size, portal vein invasion, hepatic vein invasion, tumor-node-metastasis (TNM) stage, and surgical procedure as the significant factors of the HCC morphology (Table 2). Next, the multivariate analysis was performed using the logistic regression model. As shown in Table 3, the expression of EpCAM protein ($P = 0.0092$), AFP ($P = 0.0424$), AFP-L3 level ($P = 0.0288$), and the portal vein invasion ($P = 0.0150$) were statistically independent factors of CM-type HCC.

Finally, the prognostic significance of EpCAM expression was evaluated in the patients with HCC in relation to the gross morphology. Although EpCAM expression was not associated with the patient prognosis of SN- and SNEG-type HCC ($P = 0.2193$), the significant relationship was observed between EpCAM expression and the patient prognosis in the CM-type HCC (Fig. 4A; $P = 0.0082$) or the recurrence (Fig. 4B; $P = 0.0043$). Expression of EpCAM protein might play a critical role in progression of the CM-type HCC.

TABLE 3. Multivariate Analysis for Independent Predictors of the Gross Morphology of HCC

	Odds Ratio (95% Confidential Interval)	P
AFP ≥ 100 (ng/mL)	0.360 (0.134–0.966)	**0.0424**
AFP-L3, %	1.020 (1.002–1.038)	**0.0288**
Tumor size, cm	0.981 (0.841–1.145)	0.8095
Portal vein invasion (+)	3.405 (1.268–9.143)	**0.0150**
Hepatic vein invasion (+)	1.683 (0.563–5.027)	0.3515
Tumor-node-metastasis stage		
II	1.480 (0.258–8.498)	0.6599
III	1.911 (0.279–13.108)	0.5099
IVA	1.569 (0.189–13.043)	0.6768
IVB	1.810 (0.046–71.832)	0.7521
Anatomical resection	0.612 (0.250–1.499)	0.2897
EpCAM positive	3.066 (1.319–7.125)	**0.0092**

The significance of p values in bold.

DISCUSSION

Morphological analysis of tumors has been basically used for predicting the virulent potentials.[1–6] In our present study, the gross differences of HCC were significantly associated with the clinicopathological progression, such as AFP, AFP-L3, tumor size, vessel invasion, TNM stage, and surgical procedure in SNEG and/or CM type (Table 2), resulting in poor prognosis in the patient survivals and recurrence-free survivals (Fig. 1). According to the previous reports, the vascular invasion and microscopic intrahepatic metastasis were observed more frequently in SNEG and CM types than in SN type, and that the recurrence-free survivals of SNEG- and CM-type HCC were significantly poor compared with SN-type HCC.[9,13]#12288; Our results were compatible for these studies and indicated the utility of the gross morphology of HCC to prospect for its malignant properties.

Molecular and biological features affecting the morphological phenotypes, however, have not been clarified yet in HCC. In this study, cDNA microarray technique was applied for the comprehensive analysis of gene expression signatures. Using the Kruskal-Wallis test on the microarray data, the PC analysis[25] and the hierarchical clustering[22] revealed that the SN and SNEG cases clustered together, but the CM cases were clearly distinct from the SN/SNEG cluster (Fig. 2A, B). With additional analysis of the P-value distribution using the Mann-Whitney U test,[26] the significance of differential gene expression was recognized between CM and either SN or SNEG, but not between SN and SNEG (Fig. 2C). From perspective of the gene signatures, it is noteworthy that CM-type HCC might involve essentially distinct origins from the SN and SNEG types that can progress serially. As demonstrated in Table 1, various genes were dominantly expressed in the CM-type HCC, including a stem cell marker EpCAM,[27] zinc transporter SLC39A4,[28] secreted extracellular protein CTHRC1,[29] and lipogenic enzyme ELOVL7,[30] that have been reported to overexpress in various malignancies. Our multivariate analysis revealed that EpCAM was one of the statistically independent factors of CM-type HCC (Table 3).

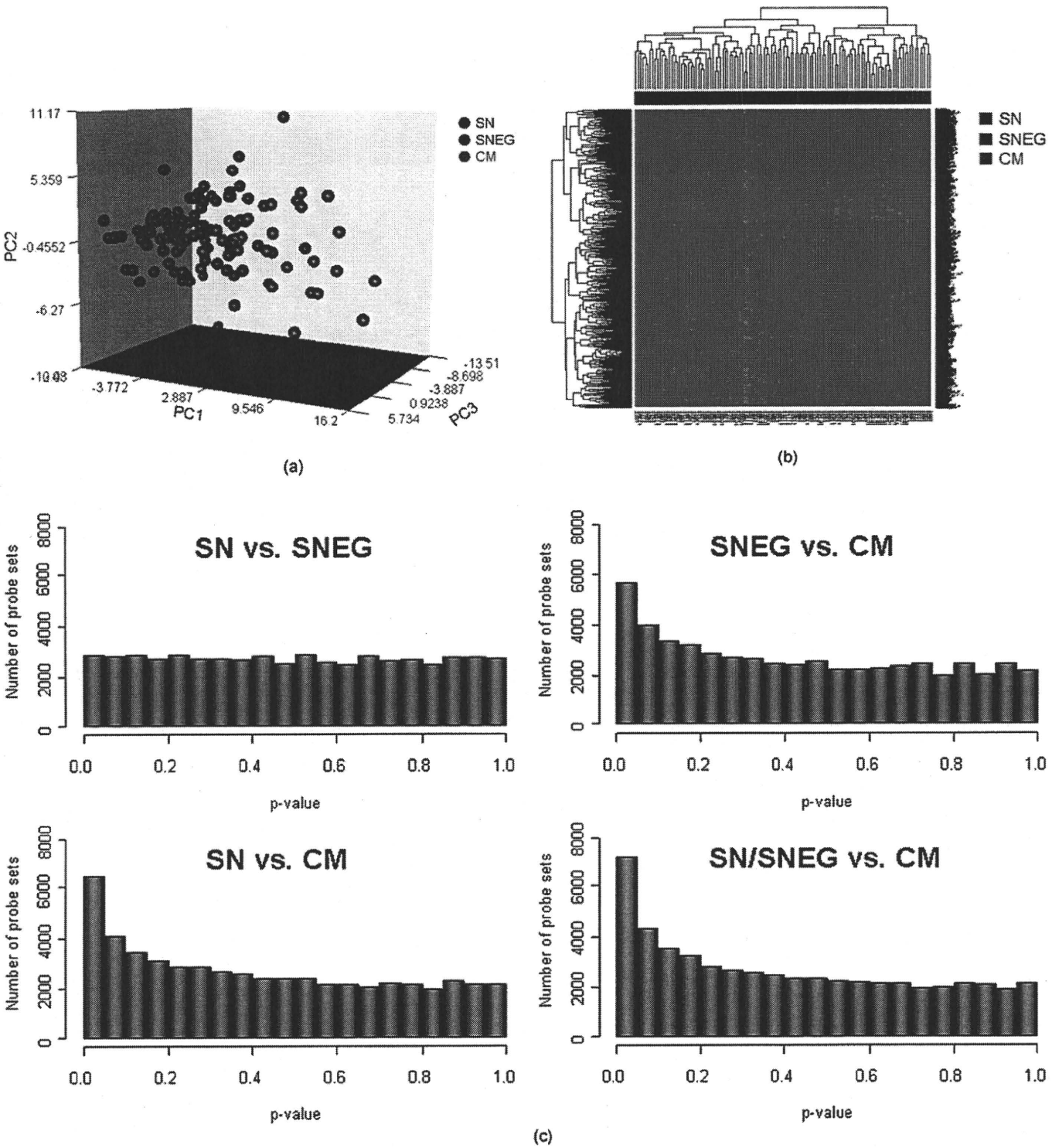

FIGURE 2. Gene expression analysis using cDNA microarray on the gross morphology of HCC. A, Scatter plots from principal component (PC) analysis of gene expression data using the Kruskal-Wallis test. PC1; the first PC, PC2; the second PC, PC3; the third PC. CM cases (red) divided from the cluster of SN (black) and SNEG cases (blue). B, Hierarchical cluster analysis of HCC in relation to the gross morphology. The distinct patterns of the gene expression in CM cases (red) compared with SN (black) and SNEG cases (blue). C, Graphical representation of the *P*-value distribution from Mann-Whitney *U* test for the gross morphology of HCC. The number of differentially expressed probe sets was demonstrated with an interval of 0.05 *P*-value. The significance of differential expression was recognized between CM and either SN or SNEG, but not between SN and SNEG.

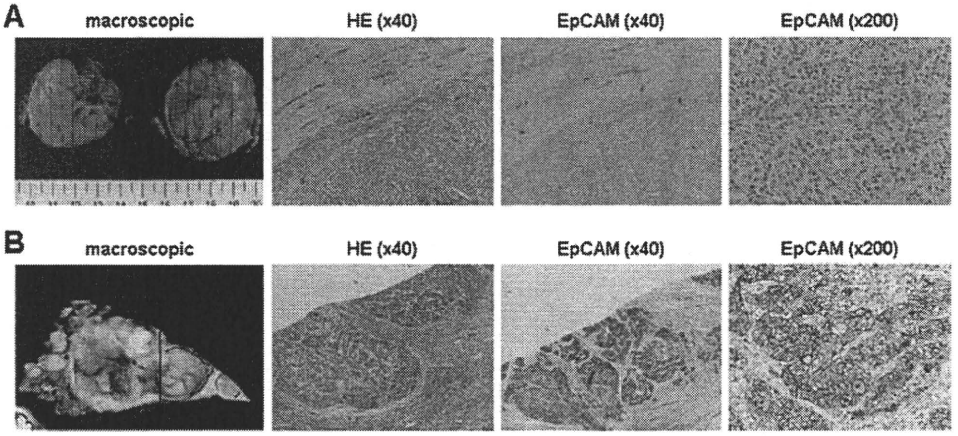

FIGURE 3. Immunohistochemical analysis of EpCAM expression in HCC cases. A, A typical SN morphology showing no EpCAM expression. B, A typical CM morphology showing EpCAM expression. Membranous staining of EpCAM in the cancer cells, but not in the adjacent noncancerous cells (magnification, ×40, ×200). HE; hematoxylin-eosin staining.

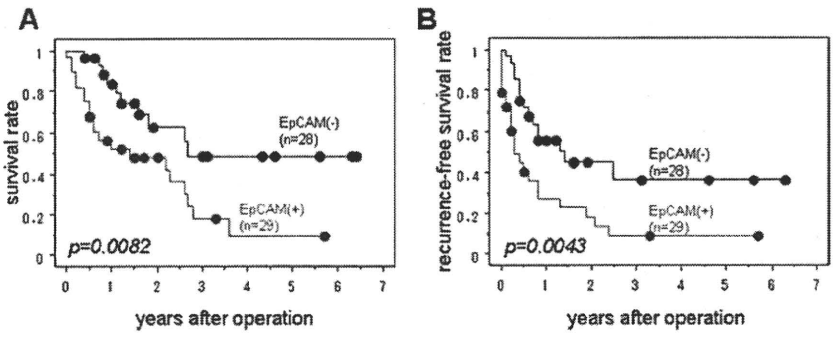

FIGURE 4. Postoperative prognosis of patients with CM-type HCC with (+) or without (−) expression of EpCAM protein. A, Overall survival curves and B, recurrence-free survival curves after curative operation. In the patients with CM-type HCC, EpCAM expression was significantly associated with the poor prognosis after curative operation ($P = 0.0082$ and $P = 0.0044$, respectively).

EpCAM, a type I transmembrane glycoprotein, has been reported to overexpress in various epithelial malignancies[31] and also known as a cancer-specific antigen 17-1A.[32] Gires and colleagues[33] revealed that EpCAM is cleaved by proteolysis on the cancer cell surface to the extracelluar ligand and intracellular domain (ICD).[33,34] The EpCAM-ICD protein directly functions as a transcriptional factor that upregulates c-myc, cyclin A, and cyclin E to promote cell cycling and proliferation.[34] Yamashita et al[35] reported that EpCAM(+)AFP(+) correlated with the poor prognosis in patients with HCC. In our study, however, the expression of EpCAM did not affect the prognosis in patients with high serum level of AFP (data not shown). On the contrary, there is a significant association of EpCAM expression with overall survival and recurrence-free survival in patients with CM-type HCC (Fig. 4; $P = 0.0082$ and $P = 0.0044$, respectively). According to recent studies by Nagrath et al,[36] the EpCAM antigen might be reliable for detection of circulating tumor cells (CTCs), suggesting EpCAM as the useful CTC marker of patients with advanced HCC, especially the CM type. Because more recent studies implied EpCAM as the biomarker for the chemoresistance of HCC,[37] the expression of EpCAM might play multiple roles in cancer progression.

Furthermore, EpCAM known as the cancer-specific antigen 17-1A has been noted as a target molecule for cancer immunotherapy.[38] Clinical trials of monoclonal antibody 17-1A (edrecolomab; Panorex) are ongoing in patients with breast, gastric, colorectal, and ovarian cancers. Recently, a trifunctional bispecific monoclonal antibody catumaxomab (Removab) has been developed for treatment of advanced cancers. Catumaxomab has 2 binding specificities directed at EpCAM and the T-cell antigen CD3, and the recent clinical phase 1/2 trials for patients with peritonea carcinomatosis or malignant pleural effusion showed a promising clinical response.[39,40] Such molecular targeting might be rational for adjuvant therapies of the EpCAM-positive HCC with CM-type.[41] Our present studies suggested not only the distinct gene signature in the CM morphology of HCC but also potentially therapeutic strategy for the aggressive phenotype in the future. Further examinations should be required to elucidate the biological significance of CM-type origination in hepatocarcinogenesis.

REFERENCES

1. Michelassi F, Vannucci L, Montag A, et al. Importance of tumor morphology for the long term prognosis of rectal adenocarcinoma. *Am Surg.* 1988;54(6):376–379.
2. Stahel RA. Morphology, surface antigens, staging, and prognostic factors of small cell lung cancer. *Curr Opin Oncol.* 1992;4(2):308–314.
3. Machado JC, Soares P, Carneiro F, et al. E-cadherin gene mutations provide a genetic basis for the phenotype divergence of mixed gastric carcinomas. *Lab Invest.* 1999;79:459–465.
4. Jaeger J, Koczan D, Thiesen HJ, et al. Gene expression signatures for tumor progression, tumor subtype, and tumor thickness in laser-microdissected melanoma tissues. *Clin Cancer Res.* 2007;13(3):806–815.
5. Montironi R, Cheng L, Lopez-Beltran A, et al. Decision support systems for morphology-based diagnosis and prognosis of prostate neoplasms: a methodological approach. *Cancer.* 2009;115(13)(Suppl):3068–3077.
6. Yang LY, Fang F, Ou DP, et al. Solitary large hepatocellular carcinoma: a specific subtype of hepatocellular carcinoma with good outcome after hepatic resection. *Ann Surg.* 2009;249(1):118–123.
7. Eggel H. Ueber das primare carcinoma der leber. *Beitz Pathol Anat.* 1901;30:506–604.
8. Kanai T, Hirohashi S, Upton MP, et al. Pathology of small hepatocellular carcinoma. A proposal for a new gross classification. *Cancer.* 1987;60:810–819.
9. Hui AM, Takayama T, Sano K, et al. Predictive value of gross classification of hepatocellular carcinoma on recurrence and survival after hepatectomy. *J Hepatol.* 2000;33:975–979.
10. Desmet VJ. East–West Pathology agreement on precancerous liver lesions and early hepatocellular carcinoma. *Hepatology.* 2009;49:355–357.

11. Choi GH, Han DH, Kim DH, et al. Outcome after curative resection for a huge (>10 cm) hepatocellular carcinoma and prognostic significance of gross tumor classification. *Am J Surg*. 2009;198(5):693–701.
12. Shimada M, Rikimaru T, Hamatsu T, et al.The role of macroscopic classification in nodular-type hepatocellular carcinoma. *Am J Surg*. 2001;182: 177–182.
13. Inayoshi J, Ichida T, Sugitani S, et al. Gross appearance of hepatocellular carcinoma reflects E-cadherin expression and risk of early recurrence after surgical treatment. *J Gastroenterol Hepatol*. 2003;18:673–677.
14. Nagano Y, Shimada H, Takeda K, et al. Predictive factors of microvascular invasion in patients with hepatocellular carcinoma larger than 5 cm. *World J Surg*. 2008;32(10):2218–2222.
15. Nakamura H, Liu T, Hori S, et al. Response to transcatheter oily chemoembolization in hepatocellular carcinoma 3 cm or less: a study in 50 patients who underwent surgery. *Hepatogastroenterology*. 1993;40(1):6–9.
16. Hashimoto T, Nakamura H, Hori S, et al. Hepatocellular carcinoma: efficacy of transcatheter oily chemoembolization in relation to macroscopic and microscopic patterns of tumor growth among 100 patients with partial hepatectomy. *Cardiovasc Intervent Radiol*. 1995;18(2):82–86.
17. Yamakado K, Nakatsuka A, Ohmori S, et al. Radiofrequency ablation combined with chemoembolization in hepatocellular carcinoma: treatment response based on tumor size and morphology. *J Vasc Interv Radiol*. 2002;13(12):1225–1232.
18. Quackenbush J. Microarray analysis and tumor classification. *N Engl J Med*. 2006;354 (23):2463–2472.
19. Iizuka N, Oka M, Yamada-Okabe H, et al. Oligonucleotide microarray for prediction of early intrahepatic recurrence of hepatocellular carcinoma after curative resection. *Lancet*. 2003;361 (9361):923–929.
20. Hoshida Y, Villanueva A, Kobayashi M, et al. Gene expression in fixed tissues and outcome in hepatocellular carcinoma. *N Engl J Med*. 2008;359(19):1995–2004.
21. Bild AH, Potti A, Nevins JR. Linking oncogenic pathways with therapeutic opportunities. *Nat Rev Cancer*. 2006;6 (9):735–741.
22. Tanaka S, Arii S, Yasen M, et al. Aurora kinase B is a predictive factor for aggressive recurrence of hepatocellular carcinoma after curative hepatectomy. *Br J Surg*. 2008;95 (5):611–619.
23. Aihara A, Tanaka S, Yasen M, et al. The selective Aurora B kinase inhibitor AZD1152 as a novel treatment for hepatocellular carcinoma. *J Hepatol*. 2010;52(1):63–71.
24. Liver Cancer Study Group of Japan. *The General Rules for the Clinical and Pathological Study of Primary Liver Cancer*. Tokyo, Japan: Kanehara; 1992.
25. Hilsenbeck SG, Friedrichs WE, Schiff R, et al. Statistical analysis of array expression data as applied to the problem of tamoxifen resistance. *J Natl Cancer Inst*. 1999;91(5):453–459.
26. Boersma BJ, Reimers M, Yi M, et al. A stromal gene signature associated with inflammatory breast cancer. *Int J Cancer*. 2008;122 (6): 1324–1332.
27. Schmelzer E, Zhang L, Bruce A, et al. Human hepatic stem cells from fetal and postnatal donors. *J Exp Med*. 2007;204:1973–1987.
28. Li M, Zhang Y, Liu Z, et al. Aberrant expression of zinc transporter ZIP4 (SLC39A4) significantly contributes to human pancreatic cancer pathogenesis and progression. *Proc Natl Acad Sci USA*. 2007;104(47):18636–18641.
29. Tang L, Dai DL, Su M, et al. Aberrant expression of collagen triple helix repeat containing 1 in human solid cancers. *Clin Cancer Res*. 2006;12(12):3716–3722.
30. Tamura K, Makino A, Hullin-Matsuda F, et al. Novel lipogenic enzyme ELOVL7 is involved in prostate cancer growth through saturated long-chain fatty acid metabolism. *Cancer Res*. 2009;69(20):8133–8140.
31. Trzpis M, McLaughlin PMJ, Leij LMFH, et al. Epithelial cell adhesion molecule. More than a carcinoma marker and adhesion molecule. *Am J Pathol*. 2007;171:386–395.
32. Went P, Vasei M, Bubendorf L, et al. Frequent high-level expression of the immunotherapeutic target EpCAM in colon, stomach, prostate and lung cancers. *Br J Cancer*. 2006;94:128–135.
33. Mastzel D, Denzel S, Mack B, et al. Nuclear signaling by tumor-associated antigen EpCAM. *Nat Cell Biol*. 2009;11:162–171.
34. Munz M, Baeuerle PA, Gires O. The emerging role of EpCAM in cancer and stem cell signaling. *Cancer Res*. 2009;69(14):5627–5629.
35. Yamashita T, Forgues M, Wang W, et al. EpCAM and α-fetoprotein expression defines novel prognostic subtypes of hepatocellular carcinoma. *Cancer Res*. 2008;68:1451–1461.
36. Nagrath S, Sequist LV, Maheswaran S, et al. Isolation of rare circulating tumour cells in cancer patients by microchip technology. *Nature*. 2007;450(7173):1235–1239.
37. Noda T, Nagano H, Takemasa I, et al. Activation of Wnt/beta-catenin signalling pathway induces chemoresistance to interferon-alpha/5-fluorouracil combination therapy for hepatocellular carcinoma. *Br J Cancer*. 2009;100:1647–1658.
38. Chaudry MA, Sales K, Ruf P, et al. EpCAM an immunotherapeutic target for gastrointestinal malignancy: current experience and future challenges. *Br J Cancer*. 2007;96:1013–1019.
39. Ströhlein MA, Siegel R, Jäger M, et al. Induction of anti-tumor immunity by trifunctional antibodies in patients with peritonea carcinomatosis. *J Exp Clin Cancer Res*. 2009;28:18.
40. Sebastian M, Kiewe P, Schuette W, et al. Treatment of malignant pleural effusion with the trifunctional antibody catumaxomab (Removab) (anti-EpCAM x Anti-CD3): results of a phase 1/2 study. *J Immunother*. 2009;32 (2):195–202.
41. Tanaka S, Arii S. Molecularly targeted therapy for hepatocellular carcinoma. *Cancer Sci*. 2009;100(1):1–8.

Abdominal Imaging

Abdom Imaging (2011)
DOI: 10.1007/s00261-011-9685-1

INVITED FEATURE SECTION

Hepatocelluar nodules in liver cirrhosis: hemodynamic evaluation (angiography-assisted CT) with special reference to multi-step hepatocarcinogenesis

Osamu Matsui, Satoshi Kobayashi, Junichiro Sanada, Wataru Kouda, Yasuji Ryu, Kazuto Kozaka, Azusa Kitao, Koichi Nakamura, Toshifumi Gabata

Department of Radiology, Graduate School of Medical Science, Kanazawa University, Kanazawa, Japan

Abstract

To understand the hemodynamics of hepatocellular carcinoma (HCC) is important for the precise imaging diagnosis and treatment, because there is an intense correlation between their hemodynamics and pathophysiology. Angiogenesis such as sinusoidal capillarization and unpaired arteries shows gradual increase during multi-step hepatocarcinogenesis from high-grade dysplastic nodule to classic hypervascular HCC. In accordance with this angiogenesis, the intranodular portal supply is decreased, whereas the intranodular arterial supply is first decreased during the early stage of hepatocarcinogenesis and then increased in parallel with increasing grade of malignancy of the nodules. On the other hand, the main drainage vessels of hepatocellular nodules change from hepatic veins to hepatic sinusoids and then to portal veins during multi-step hepatocarcinogenesis, mainly due to disappearance of the hepatic veins from the nodules. Therefore, in early HCC, no perinodular corona enhancement is seen on portal to equilibrium phase CT, but it is definite in hypervascular classical HCC. Corona enhancement is thicker in encapsulated HCC and thin in HCC without pseudocapsule. To understand these hemodynamic changes during multi-step hepatocarcinogenesis is important, especially for early diagnosis and treatment of HCCs.

Key words: Hepatocellular carcinoma—Blood supply—Multi-step hepatocarcinogenesis—Early HCC—Dysplastic nodule—Liver

Hepatocellular carcinoma (HCC) is the most common primary liver cancer worldwide. Approximately 80% of Japanese HCC cases are derived from HCV-associated liver cirrhosis and chronic hepatitis, and the remaining less than 20% of the patients are HBV positive. The patients with hepatitis B or C cirrhosis are especially classified as a very high-risk group. Ultrasonography is performed every 3–4 months for the very high-risk group. Because of the introduction of this surveillance system, the size of HCCs firstly detected during 2002–2003 (n = 33731) was less than 2 cm in 32.5% of all cases, 2.1–5.0 cm 47.0%, respectively [1]. However, various types of hepatocellular nodules such as dysplastic nodule (DN) are also detected during screening procedures. Ultrasound and CT features of DNs and early HCCs are similar, and a precise differential diagnosis is impossible. Pathologically, human HCC develops in a multistep fashion from DN to classic hypervascular HCC. Therefore, for the early diagnosis of HCC, understanding of the concept of multi-step hepatocarcinogenesis and the sequential changes of imaging findings in accordance with multi-step hepatocarcinogenesis is important.

To understand the hemodynamics of HCC is important for the precise imaging diagnosis and treatment, because there is an intense correlation between its hemodynamic and pathophysiology. For this purpose, dynamic MDCT is most valuable because of its high

Correspondence to: Osamu Matsui; *email:* matsuio@med.kanazawa-u.ac.jp

Published online: 26 January 2011